AALBORG
UNIVERSITY

STUDENT REPORT

AALBORG UNIVERSITY
DEPARTMENT OF MATERIALS AND PRODUCTION

MATERIALS AND NANOTECHNOLOGY: MATERIALS TECHNOLOGY

MASTER'S THESIS

Structure–Property Relations for Recycled HDPE at Large Deformations in the Liquid State and Effect on Crystallization

MAJA H. MIKKELSEN

31/05-2024

AALBORG
UNIVERSITY

STUDENT REPORT

Department of Materials and Production /
Study Board of Physics and Mechanics
Aalborg University
www.mp.aau.dk

Title:

Structure–Property Relations for Recycled HDPE at Large Deformations in the Liquid State and Effect on Crystallization

Semester:

4th Semester Materials Technology

Semester theme:

Master's Thesis

Project period:

February 2024 - June 2024

ECTS:

30

Supervisor:

Jesper de Claville Christiansen

Secondary Supervisor:

Aleksey D. Drozdov

Participants:

Maja H. Mikkelsen

Page numbers: 42
Appendices page numbers: 15
Date of Completion: May 31, 2024

Abstract:

This thesis investigated the changes to the degree of crystallinity and structure of HDPE as a result of thermo-oxidative degradation. The aim of this investigation was to characterize the relationship between the internal structure of recycled HDPE and increased sensitivity seen in cyclic loading failure. The thermal, rheological and optical properties of virgin HDPE (vHDPE), degraded vHDPE (vHDPEdeg280) and post-consumer recycled HDPE (rHDPE) were investigated by TGA, DSC, OIT, rheology, solvent swelling, FTIR, optical microscopy and SEM. The results of thermal testing yielded a decrease in the degree of crystallinity for degraded samples, as well as an increase in the degradation temperature seen by TGA. Large amplitude oscillatory shear rheology (LAOS) was found to be an effective method of characterizing the changes in the behavior of the internal structure of the HDPE melt as a result of degradation. Optical microscopy and SEM highlighted the complex effects of degradation on the crystalline structure, showing greater inhomogeneity of the crystalline structure for degraded samples. The effects of degradation on HDPE were investigated through LAOS and crystallinity analysis, showing clear changes to the internal structure as a result of complex degradation mechanisms.

Preface

The following Master's thesis was written by Maja Hirschel Mikkelsen, 4th semester Materials Technology at Aalborg University under the supervision of Professor Jesper de Claville Christiansen. The project period was from the 1st of February 2024 to the 31st of May 2024.

The premise of the project was presented in relation to the RHQI project #9091-00010B at Aalborg University along with a previous student project and previous papers published on the subject at AAU.

In this project the structure-property relations of virgin and recycled HDPE were investigated through the degree of crystallinity and large amplitude oscillatory shear rheology. The scope of this project was limited to testing of rheological, thermal and optical properties of virgin and recycled HDPE, as the mechanical properties of the materials used have been previously investigated.

Tables, figures and equations are numbered in order of appearance. Citations are listed in alphabetical order with [citation number]. Full references are shown in the bibliography.

Acknowledgements are given to my supervisor for help and guidance in theories and testing parameters. Furthermore, the laboratory team at Fibigerstræde 14 has been instrumental in assistance with testing setup. Special thanks to Ahunik Mesropovna Asatarjan and Anne Louise Olsen for sparring and support.

Maja Hirschel Mikkelsen

Summary

This thesis investigated the causes of deteriorated fatigue properties of HDPE found in cyclic loading of virgin (vHDPE) and recycled HDPE (rHDPE). Through previous investigation of the cyclic loading mechanisms of vHDPE and rHDPE, cyclic loading was established as a more sensitive test method for observing changes to the mechanical behavior of rHDPE, compared to uniaxial tensile testing. These results were corroborated by published papers examining the viscoelastic behavior of vHDPE and rHDPE in creep and relaxation tests. The aim of the investigation in this thesis was to examine the relations between the structure of recycled HDPE and the corresponding mechanical, thermal and rheological properties. This was done in order to build an understanding of why test methods relating to slow crack growth show greater differences between vHDPE and rHDPE.

The degradation mechanisms of HDPE were found in literature to be a complex combination of chain scission, chain branching and crosslinking. The molecular chain architecture changes as a result of degradation, with decreased molecular weight (MW) by chain scission, interruptions to chain linearity by chain branching and physical links between chains leading to an increase in MW by crosslinking. As a result, effects of degradation are visible in both crystalline and amorphous regions of a polymer. The entanglement density increases as a result of chain branching and crosslinking, but decreases as a result of chain scission. As a result, degradation where crosslinking and chain branching are dominant tends to decrease the degree of crystallinity, whereas degradation with primarily chain scission tends to increase the degree of crystallinity.

The results of thermal testing by thermogravimetric analysis (TGA), differential scanning calorimetry (DSC) and oxidation induction time (OIT) were analysed with respect to changes in the degradation temperature and the degree of crystallinity. Non-colored HDPE oxidized at increasing temperatures prior to TGA and DSC showed slightly increasing degradation temperatures in TGA, as well as decreasing crystallinity from DSC. These results correspond primarily to the effects resulting from crosslinking and chain branching found in literature. Additional effects to the crystalline structure were observed in microscopy of virgin and degraded samples, where degradation corresponded to greater inhomogeneity of the sample surface.

LAOS was found to be an effective tool in describing the structural behavior of virgin, recycled and degraded HDPE as a result of high shear rates. The results of LAOS amplitude sweeps showed increased non-linearity of degraded vHDPE compared to vHDPE. These effects were especially clear at high frequency amplitude sweeps, where the brittle behavior of the internal structure was enhanced. Thermo-oxidative degradation, typically associated with recycling, on the structural properties of HDPE was found to have a clear effect on the behavior of the internal structure when analysed through crystallinity and LAOS.

Nomenclature

Abbreviations

DSC	Differential Scanning Calorimetry
ESC	Environmental Stress Cracking
FTIR	Fourier-transform infrared spectroscopy
HDPE	High Density Polyethylene
LAOS	Large Amplitude Oscillatory Shear
MW	Molecular Weight
MWD	Molecular Weight Distribution
SAOS	Small Amplitude Oscillatory Shear
SCG	Slow Crack Growth
SEM	Scanning Electron Microscopy
TGA	Thermogravimetric Analysis

Symbols

ΔH_m	Enthalpy of melting
δ	Phase angle
η^*	Complex viscosity
τ	Shear stress
G''	Loss modulus
G'	Storage modulus
T_c	Crystallization peak temperature
T_g	Glass transition temperature
T_m	Melting peak temperature
X_c	Degree of crystallinity

Contents

1 Introduction

In 2022, the global plastics production surpassed 400 Mt, spurred on by a constantly increasing demand for plastic products for industrial and household use [57]. Among this, only 8,9% was sourced from mechanically recycled plastic. In order to comply with EU restrictions on the production of virgin plastics, while simultaneously fulfilling the high demand for plastic products, the use of recycled plastics is a prominent topic [53]. High density polyethylene accounts for 12% of the global plastic production yearly, with applications in both household products, such as detergent bottles, and industrial products, such as gas-transporting pipes [33]. HDPE for industrial use has strict requirements, due to the importance of a highly dependable service lifetime. As a result, the use of recycled HDPE necessitates thorough analysis of the effects of degradation on structural properties.

1.1 Project description

The base of this thesis stems from a previous student project investigating the cyclic loading properties of virgin and recycled HDPE titled: "Characterization of Properties of Virgin and Recycled High-Density Polyethylene under Cyclic Loading" [4]. Through mechanical testing of vHDPE and rHDPE, it was evident, that testing of fatigue properties via cyclic loading revealed greater differences between virgin and recycled HDPE, compared to classical uniaxial tensile testing. Similar results relating to slow crack growth (SCG) mechanisms were observed in [20, 24].

Cyclic loading of HDPE was shown to be a more sensitive testing method than tensile testing with recycled HDPE failing earlier than virgin HDPE [4]. Similar effects were seen in environmental stress cracking (ESC) of HDPE [13, 15, 16, 29, 58, 64]. As both fatigue and ESC failure are dominated by SCG, an interesting question is posed:

Why are fatigue properties and SCG more effective at distinguishing differences between vHDPE and rHDPE?

Possible causes of this are differences in crystallinity, network and entanglements. This thesis aims to investigate these causes through large amplitude oscillatory rheological tests (LAOS) and differential scanning calorimetry (DSC). LAOS was used to examine the HDPE melt in the non-linear viscoelastic region, to understand the behavior of the network under large deformations. DSC was used to examine the crystallinity under controlled heating and cooling cycles.

According to Yin et al. [66], the worsening of mechanical properties of polyolefin wastes are primarily due to degradation and contamination. Exposure of HDPE pipes to HCl environments and distilled water in [28] led to degradation of the pipe surface and changes in crystallinity. Through testing of mechanical reprocessing, Zeng et al. [69] cataloged increasing surface roughness and higher porosity of recycled HDPE.

Tie molecules in the interfaces between amorphous and crystalline regions of polyethylene were

found by Lustiger and Markham [43] to be highly influential in fracture behavior. The fracture of polyethylene was further influenced by molecular weight, degree of crystallinity, lamellar orientation and branching.

As explored in literature pertaining to the structure and degradation of HDPE, the polymeric structure of HDPE is important to investigate, in order to correlate structure to the previously characterized mechanical properties. In order to minimize the effects of contaminants on the structural properties, controlled thermo-oxidative degradations of virgin HDPE are performed to simulate degradation caused by recycling. This thesis investigates the thermal, rheological and optical properties of virgin, recycled and virgin-degraded HDPE, in order to determine their effects on the mechanical properties catalogued in [4], which are further described in section 2.4.

This is done by the following methods:

- Preparation of degraded and virgin HDPE discs, using an AR-G2 parallel plate rheometer, to compare the changes to crystallinity and macromolecular structure
- DSC of each batch to determine the effects of degradation on the degree of crystallinity
- Oxidation Induction Time (OIT) testing to verify the effects of degradation at the chosen temperatures
- Swelling tests of HDPE discs in Arkopal and xylene to map the diffusion of different solvents into the structure
- LAOS rheological testing to investigate the rheological properties resulting from deformation of the melt in the non-linear viscoelastic region
- Scanning Electron Microscopy (SEM) and optical microscopy on etched HDPE discs to visualize effects of controlled degradation on the structure of crystalline regions

2 Background Theory

The following chapter describes the theoretical background of the investigations in this thesis.

2.1 Polyethylene

High density polyethylene (HDPE) is a semi-crystalline thermoplastic polymer with a highly linear chain structure, as seen in figure 1. Due to the linearity of its polymer chains, the crystallinity of HDPE is often high.

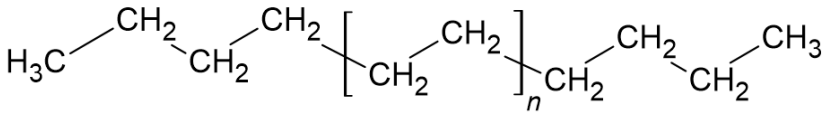

Figure 1: Structure of Polyethylene

Highly crystalline polymers have high chemical resistance and toughness, due to the protection of crystalline regions against solvent diffusion, presenting them as excellent candidates for industrial products. As a result, HDPE is extensively used in gas- and fluid-carrying pipes, due to its chemical resistance and toughness [12].

Effect of additives

Carbon black is a black pigment often used as a UV stabilizer and oxidation protectant for polymers, especially in pipe material, as it prevents light from penetrating the polymer [46]. Poor dispersion of carbon black can have detrimental effects on the mechanical properties of polyethylene pipes, as it can act as an initiation point for crack growth. This was demonstrated by Deveci et al. [21], where worsened fracture properties were observed as a result of increased heterogeneity of carbon black distribution in polyethylene pipes. Similarly, Alavifar et al. [2] observed deteriorated resistance of PE-100 pipe material to SCG due to poor carbon black dispersion and the presence of low MW substances in the structure. A homogeneous carbon black distribution yielded a strengthened polymer network within the amorphous regions with high resistance to SCG.

2.2 Degradation of HDPE

During mechanical recycling of HDPE, possible changes to the molecular architecture, due to degradation, must be taken into account.

Alzerreca et al. [3] examined the mechanical behavior and the effects of molecular structure, fillers and contaminants in the recycling of HDPE, in order to improve the quality of recycled HDPE. The analysis of PCR HDPE revealed unacceptable long-term performance, attributed to a lack of tie molecules and shortened chain lengths. The proposed improvements in [3] were a

reduction of the amount of contaminants, as well as an improvement of sorting and recycling processes of HDPE to increase the amount of tie molecules.

Mendes et al. [45] found that the degradation of polyethylene occurs by competing mechanisms of chain scission and crosslinking. Pinheiro et al. [56] similarly observed that the degradation effects of HDPE were worsened with an increasing number of extrusion cycles, as well as increases in temperature.

Cruz and Zanin [18] observed crosslinking in PCR HDPE, highlighting the necessity of a stabilizer when reprocessing. Left-over impurities from polymerization catalysts were hypothesized to lead to increased degradation, due to contaminants and reactive end-groups.

Holmström and Sörvik [34] investigated the structural changes of HDPE under thermal and thermo-oxidative degradation. Increases in oxygen content, exposure time and temperature led to increases in degradation products, long chain branching and low MW products. An insoluble fraction was simultaneously observed, indicating the presence of crosslinking. The results presented in [34] highlight the complex degradation mechanisms of HDPE, as well as their fluctuations according to degradation method parameters.

The authors of [50] focused on the examination of mechanical, rheological and thermal properties of HDPE, as a result of 100 consecutive extrusion cycles, monitoring processing conditions simultaneously. The methods applied showed chain scission and side chain branching as the primary competing degradation mechanisms, occurring simultaneously from the first reprocessing cycle. Additionally, degradation by crosslinking became evident, as reprocessing progressed above 60 cycles. The processability of HDPE was negatively affected within the first 10 cycles, whereafter reevaluation of processing parameters were necessary. The deterioration of mechanical properties was not evident before 10 reprocessing cycles [50].

The investigations of mechanical reprocessing of polyolefin waste by [66] showed the effects of processing parameters on the properties of recycled HDPE waste materials. A lamellar orientation perpendicular to the direction of stress was found to be more likely to lead to interlamellar failure, compared to an orientation parallel to the direction of stress. Additionally, as MW increased, correlating to longer polymer chains, the amount of tie molecules and effective entanglements increased, increasing the resistance of HDPE to SCG and ESC.

2.3 Polymer structure

The structure of a polymer can be comprised of different regions with different arrangement of polymer chains, each with unique properties and effects on the mechanical behavior. These regions are characterized by amorphous structuring of polymer chains, seen in figure 2a and crystalline structure, seen in figure 2b, with interfacial regions separating them.

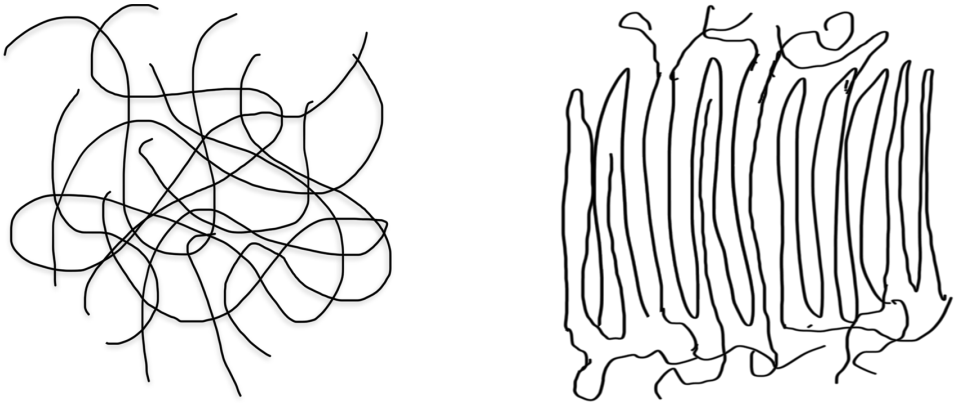

(a) (b)

Figure 2: Molecular configuration of amorphous (a) and crystalline (b) polymer chains

Crystalline zones in a polymer are characterized by densely packed, ordered polymer chains in lamellar structures. Crystalline domains lie among randomly coiled chains, resulting in a lamellar structure in semi-crystalline polymers. Amorphous regions lie between crystalline zones in the polymer, where the packing of chains is chaotic and lacking regularity. Between the amorphous and crystalline phases is an interface, with properties that are not fully crystalline or amorphous. The behavior and structure of polymer chains is dependent on the thermal history which the polymer has been exposed to.

Upon cooling, crystallization initiates from randomly distributed nucleation points in the melt. Nucleation points are typically impurities, nucleating agents or filler particles. As crystallization proceeds, lamellae distribute around the nucleation points, resulting in a spherulitic structure. The growth of each spherulite is interrupted by the boundary of surrounding spherulites [31].

The size and architecture of crystalline regions is controlled by [31]

- chain architecture
- MW and MWD
- additives and contaminants
- pressure and shear force

Schrauwen et al. [60] found a dependency between the entanglement density of the amorphous phase in semi-crystalline polymers and the large-strain deformation behavior. Strain hardening of semi-crystalline polymers is controlled by the entangled polymer network of the amorphous phase.

In the analyses performed by Bartczak and Kozanecki [7], yielding behavior was found to be dependent on both the ratio of amorphous to crystalline regions and the size of crystallites, specifically the lamellar thickness. However, strain hardening behavior was found to be primarily

dependent on the entanglement density in the amorphous component. Entanglement density is dependent on the chain architecture and MW of the polymer, which influence the folding of chains into a network structure during crystallization [7].

Entanglements at the edges of amorphous regions, bridging crystallites, define physical crosslinks in the polymer network, as some entanglements become "trapped" by the crystal structure. These types of entanglements are often referred to as tie molecules [43]. The mechanical behavior of a semi-crystalline polymer is affected by the structure of both the crystalline and amorphous regions, as well as the interfaces between them. Chains outside of the crystalline regions have a high level of entanglement, and connect the crystalline regions with tie molecules, loops or tails [8].

A higher prevalence of molecular disentanglements can lead to a decrease in the structural strength of polymers, resulting in faster failure [47]. The investigations of HDPE types with different molecular weights in [22] found, that a higher MW was conducive to a more regular crystalline structure, slowing the viscoelastic processes of creep and relaxation.

Cheng et al. [15] investigated the effects of the crystalline phase of polyethylene on the environmental stress cracking resistance (ESCR) with a focus on an analysis of the degree of crystallinity and lamellar thickness. An increased lamellar area was found to improve ESCR, due to an increase in the prevalence of interlamellar links, with SCB hindering the formation of lamella. MW and chain structure were also determined to affect the crystallinity of HDPE, by testing different grades of HDPE produced using identical processing conditions.

Pagès et al. [52] studied the structural and mechanical changes in HDPE which was exposed to ageing by weathering, finding a decrease in crystallinity as ageing time increased.

Zeng et al. [69] observed a correlation between increased surface roughness and a decrease in crystallinity in mechanically recycled HDPE. The investigation focused on the microstructure and morphological properties of virgin HDPE, PIR HDPE and PCR HDPE, and found, that the properties of PCR HDPE were significantly reduced compared to virgin HDPE. Bartczak and Vozniak [8] studied the influence of topology of the amorphous phase on lamellar fragmentation and deformation instabilites. Deformation behavior of semi-crystalline polymers, studied in [60], revealed that strain hardening is controlled primarily by the chain entanglement density, and is not influenced by the crystalline phase.

The investigations of thermal degradation of crosslinked HDPE performed by Han et al. [32] highlighted a link between the degradation of HDPE and the degree of crystallinity, where thermal oxidation led to an increase in the amorphous phase, and thus a decrease in the degree of crystallinity. A similar decrease in the degree of crystallinity of recycled HDPE, observed by Zeng et al. [70], was found to increase the formation of amorphous regions, due to irregularity in the arrangement of chains compared to vHDPE. Additionally, the crystallization behavior of rHDPE was interrupted by contaminants and oxidation products, yielding longer crystallization times. Thus, [70] concluded that melt processing of rHDPE necessitates sufficiently high temper-

atures, along with lowered interfacial tension to account for increased surface roughness from contaminants.

2.4 Slow Crack Growth (SCG)

Failure due to high stresses occurs by ductile failure mechanisms, where cracks propagate rapidly in a deformation zone [36]. In contrast, failure caused by low stress loading results in brittle failure by SCG. Testing of the SCG mechanisms are often done by long-term testing, such as creep and ESC, or fatigue testing, where deformation of polymer chains occurs gradually, due to disentanglement and slippage of the molecular structure of a polymer.

The viscoelastic response of HDPE under creep conditions was investigated in [23], accounting for slip mechanisms in failure from disentanglement and sliding of tie chains in the amorphous region, as well as lamellar slipping in crystalline regions.

Cazenave et al. [13] found that the strength of the macromolecular network of polyethylene is controlled by intercrystalline tie molecules, which provide resistance against SCG and ESC.

Environmental Stress Cracking (ESC)

The initiation of ESC occurs by craze formation, resulting from disentanglement and slippage of the polymer chains. Exposure of a material to chemical environments accelerates the disentanglement mechanism in ESC [17]. In the crystalline regions, the polymer chains are tightly packed and form ordered crystalline zones, which function as a barrier, hindering diffusion of a given chemical, into the molecular structure. Thus, the amorphous region of semi-crystalline polymers has a higher susceptibility to ESC compared to the crystalline region. As a chemical diffuses into the amorphous regions of the polymer, it results in a reduction of the intermolecular forces. This can cause molecular slippage and crazes, enabling crack propagation and eventually failure.

Properties affecting ESC [17]:

- Degree of crystallinity
- MW and MWD
- Additives
- Chemical factors and affinity
- Stress (applied and residual)
- Environmental conditions (UV, temperature, time etc.)

ESC agents with a mild to moderate affinity toward a polymer, result in insignificant changes to the polymer under unstressed immersion. Chemicals with a strong affinity towards a polymer

will diffuse into the structure in unstressed conditions. In stressed conditions, the molecular orientation of polymer chains changes, due to interactions between intermolecular forces and the applied stress. As chains are pulled apart under stress, the localized free volume between chains increases, allowing chemical agents with lower attraction to diffuse into the polymer structure [17].

Qin et al. [58] investigated the changes in physical structure of polyethylene pipes, leading to failure by ESC, where the authors studied the changes in phase structure, molecular mobility and relative sizes of the amorphous and crystalline domains. According to the investigations of ESC in HDPE in [64], solvent interaction in ESC leads to localized plasticization around the crack initiation point, accelerating crack propagation.

Gobetti and Ramorino [29] performed short-term thermal and mechanical tests using commercially well-known test methods. Through these test methods, the effect of recycling of HDPE on ESCR was researched using 8 different types of recycled HDPE. According to [29], the main polymer characteristics responsible for improvement of ESCR are tie molecules and entanglements.

Investigations performed by Cheng et al. in [15, 16] found that interlamellar links are critical in resistance to ESC. Phase interconnectivity between the amorphous and crystalline regions was found to be critical to the resistance against ESC, with larger crystalline areas having favorable protection against ESC. Network mobility was an important factor in SCG, with higher MW providing increased chain entanglements, limiting the mobility of the polymer network.

Lustiger and Markham [43] concluded that ESC of HDPE occurs by an accelerated brittle SCG mechanisms similar to the failure mechanisms present in long-term tests in air.

Cyclic Loading Fatigue

The investigation of fatigue fracture by Andrews and Walker [5] showed a correlation between the size of polyethylene spherulites and fatigue life related to intrinsic flaws initiating cracks.

According to Jo et al. [40], the deformation-induced non-linear viscoelasticity of oriented HDPE specimens under fatigue conditions stems from the interfacial properties between the amorphous and crystalline regions, instead of solely the crystalline region.

The viscoelastic response of HDPE in creep and the investigations of tensile, relaxation and creep properties for vHDPE and rHDPE in [24] revealed little changes to tensile properties due to recycling. Ductile failure of rHDPE and vHDPE under creep conditions yielded only slightly greater differences than tensile testing.

The fatigue properties of HDPE were investigated in [11], highlighting the dependence of the accumulated damage on the loading mechanism and the level of loading.

The authors of [20] investigated the mechanical properties of vHDPE and rHDPE in terms of

tensile properties, relaxation, creep and fatigue. Their results showed that rHDPE exhibited a decreased resistance to creep, with more evident differences in the fatigue properties at low strain rates. Similar tensile trends were observed in [71], with faster failure of rHDPE under fatigue loading conditions, compared to vHDPE.

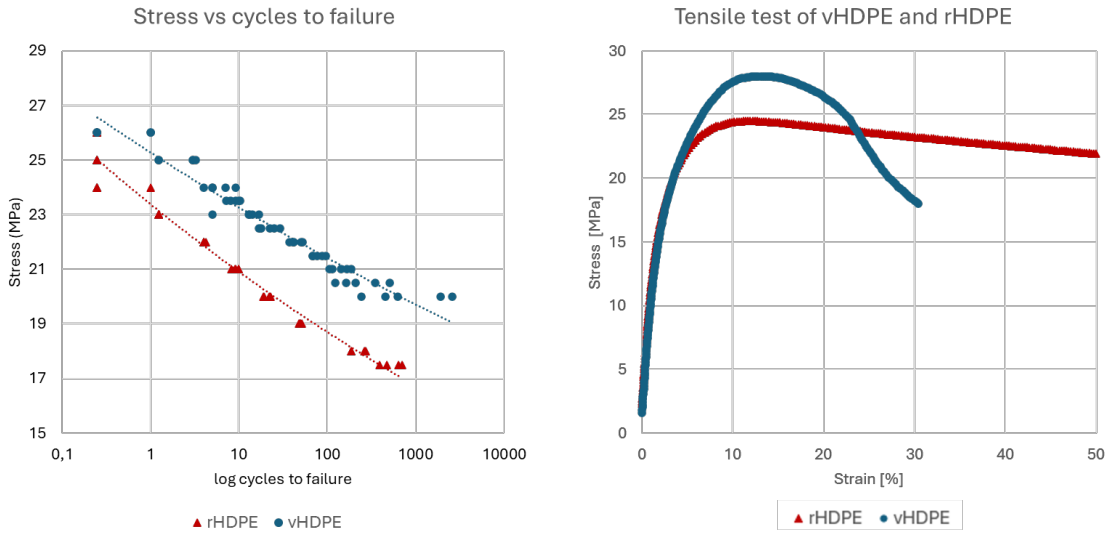

(a) Semi-logarithmic S-N curve of vHDPE and rHDPE under cyclic loading

(b) Stress-strain curve of vHDPE and rHDPE in a tensile test

Figure 3: Cyclic loading and tensile test of vHDPE and rHDPE adapted from [4]

Comparison of cyclic loading fatigue and uniaxial tensile testing of vHDPE and rHDPE in [4] revealed greater differences in fatigue properties than tensile properties, aligning with the results seen in literature. Figure 3a shows the differences in S-N curves of the fatigue lifetime of vHDPE and rHDPE. At longer cycles-to-failure, the differences between vHDPE and rHDPE were amplified. Calculations of the theoretical 50-year service lifetime based on the applied model revealed a 36% lower fatigue strength of rHDPE compared to vHDPE. In comparison, the tensile strength of rHDPE compared to vHDPE, found in the investigation of uniaxial tensile properties only yielded approximately 14% decrease.

2.5 Rheology

Polymer melts exhibit shear thinning viscoelastic behavior, with increasing shear rates, resulting in decreasing viscosity.

In parallel plate oscillatory rheology, a polymer melt is oscillated between two plates, resulting in a sinusoidal relation of the applied shear stress, τ and resulting shear strain, γ, seen in figure 4. The shift between the stress and strain gives the phase angle δ.

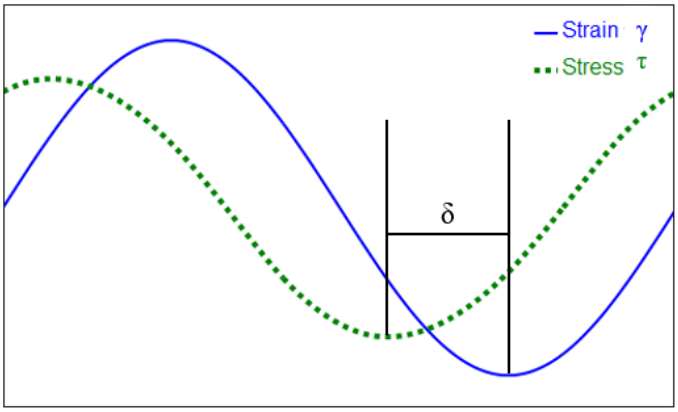

Figure 4: Stress-strain relation of SAOS

The stress and strain can be related to the storage modulus, G', which describes the elastic behavior, and the loss modulus G", which describes the viscous behavior. These relations can be seen in equation 1 [47].

$$G' = \frac{\tau}{\gamma} \cdot cos(\delta) \qquad G'' = \frac{\tau}{\gamma} \cdot sin(\delta) \tag{1}$$

Based on the relations between G' and G", the complex viscosity, η^*, which describes the viscoelastic flow properties in rheological testing, can be defined by equation 2:

$$|\eta^*| = \sqrt{\left(\frac{G'}{\omega}\right)^2 + \left(\frac{G''}{\omega}\right)^2} \tag{2}$$

The elastic behavior of a polymer melt is affected by the deformation rate and temperature. At high shear rates and high frequency, elastic behavior becomes more dominant. Similarly, the mobility of the molecular network is limited, as the temperature decreases. High temperatures and small deformations increase the mobility of molecular networks, promoting the viscous flow behavior of the polymer melt [47]. Within the linear viscoelastic (LVE) region , the stress-strain response can be represented by a sinusiodal relation. The limitation of the LVE region is defined for polymer melts by ISO 6721-10, as a 5% change in G', G" or G* [47]. This change from linear to non-LVE behavior is exemplified in figure 5, where the initial greyed portion of the amplitude sweep indicates the LVE region.

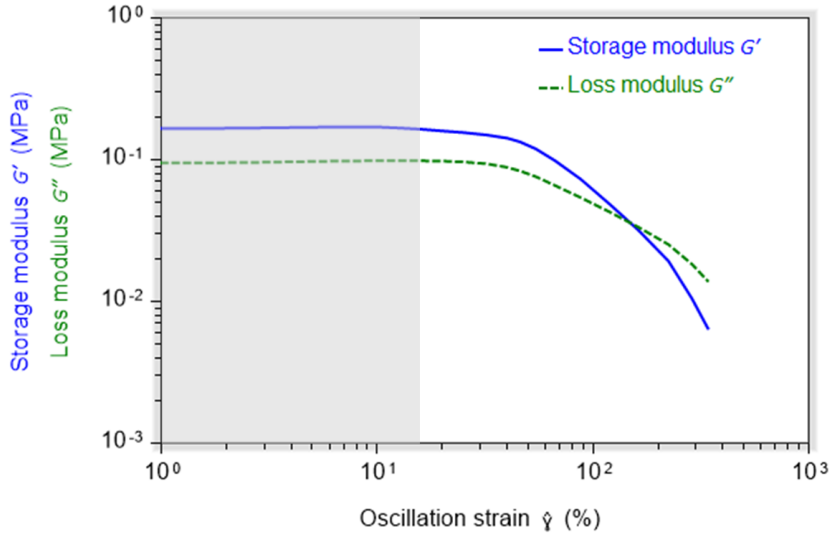

Figure 5: Schematic representation of G' and G" in an amplitude sweep

The LVE region of an amplitude sweep can be used to define a strain amplitude for further testing of rheological properties in a frequency sweep. The crossover point of G' and G" in a frequency sweep within the LVE region, can indicate changes to the weight average molecular weight (MW) and the molecular weight distribution (MWD). This relation is represented in figure 6, where shifts of the crossover point up or down correlates to a narrower or broader MWD, respectively. Similarly, shifts of the crossover point left indicate an increase in MW, while shifts to the right indicate a decrease in MW [1, 47].

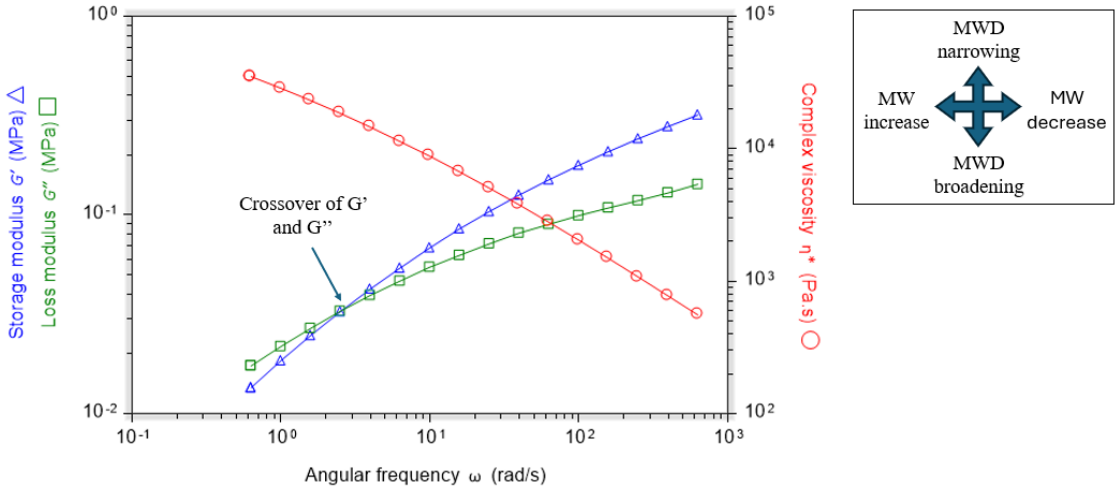

Figure 6: Schematic representation of the crossover point of G' and G" in a frequency sweep

This relation can be used to characterize effects of possible degradation, as crosslinking tends to increase the MW, while chain scission tends to decrease the MW [41].

Large Amplitude Oscillatory Shear (LAOS)

The principles of linear viscoelasticity are only valid for small deformations. However, during processing, the polymer melt is exposed to large, rapid deformations, and thus exhibits non-LVE behavior. The limit of linearity, referred to as the yield point, τ_y, is the shear stress, at which the polymer diverges from the LVE region. As shear further increases, the viscous flow behavior begins to dominate, marked by the crossover $G' = G''$ in an amplitude sweep. This crossover is called the flow point, τ_f [47]. This non-linear behavior can be predicted using large amplitude oscillatory shear (LAOS), as a tool to distinguish between structural differences. An increase in molecular disentanglements can be correlated to a decrease in the structural strength associated with polymers [47].

At small strains in the LVE region, with constant G' and G", the polymer melt is described by entangled chains. As strain increases above the LVE region, the network structure is compromised, and chains become disentangled. At large shear strain amplitudes, the response of shear stress is no longer sinusoidal, and is instead comprised of higher harmonics [62].

Lissajous-Bowditch plots, represented by a stress-strain hysteresis loop, are commonly used as a prediction of non-linearity, as testing within the LVE region results in an even ellipsoidal plot, seen in figure 7a. The area of the hysteresis loop represents the energy dissipation. As the LVE region is exceeded, both the viscous and elastic behavior of the material change, resulting in deviation from the ellipsoidal shape and an irregularly shaped hysteresis loop, as seen in figure 7b.

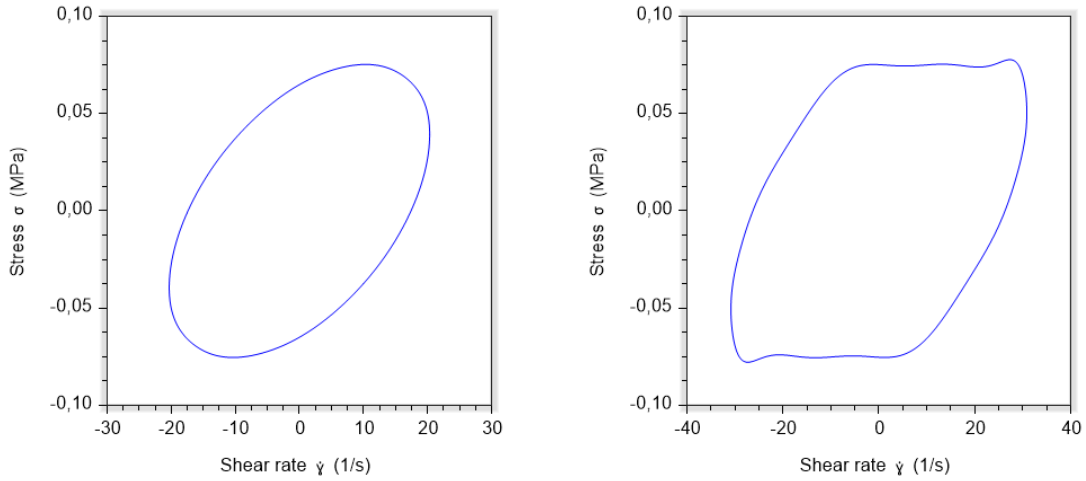

(a) Hysteresis loop in the linear region (b) Hysteresis loop in the non-linear region

Figure 7: Linear and non-linear stress-shear rate Lissajous-Bowditch plots

A method of LAOS analysis for supramolecular structures and polymer solutions and melts was developed by Ilyin et al. [38]. Chen [14] applied LAOS to branched polyethylene, to characterize structural changes, resulting from a higher degree of branching. Jeyaseelan and Giacomin [39] investigated LAOS of a filled polymer melt, finding that the strain amplitude had a strong effect

on the non-linearity of carbon black filled polyethylene. The conclusions drawn in [39] are dependent on the assumption that filler materials in a polymer melt have no direct influence on the kinetic behavior of the chain entanglement.

3 Materials and Methods

This chapter introduces the materials and methods utilized in investigation of the points described in section 1.1.

3.1 Materials

The virgin HDPE used for rheological and thermal testing was Borsafe HE3490-LS from Borealis. This HDPE grade, referred to in this thesis as vHDPE, is a pipe grade HDPE containing carbon black, and exhibits excellent rapid- and slow- crack growth properties [10]. For continuity of comparison with a recycled HDPE, PE-HD-R-E-GREY from Aage Vestergaard Larsen was used. This is a bottle grade post-consumer recycled HDPE, referred to in this thesis as rHDPE. The virgin and recycled HDPE, vHDPE and rHDPE, used in this thesis correspond to the batches used in testing of vHDPE and rHDPE used in [4, 24].

A second virgin HDPE type, Eraclene MP90 from Versalis, was used for testing of optical properties. This HDPE grade was also used for additional testing of thermal properties, as well as swelling. Eraclene MP90, referred to in this thesis as uHDPE, is a non-colored injection molding HDPE grade, with antioxidants with excellent thermal stability and high rigidity [65].

(a) vHDPE (b) rHDPE (c) uHDPE

Figure 8: vHDPE, rHDPE and uHDPE pellets

The materials used for individual tests, as well as the form used, are listed in table 1.

	vHDPE	rHDPE	uHDPE
DSC (disc)	x	x	x
OIT (pellet)	x		x
Rheology (pellets)	x	x	
TGA (disc)	x	x	x
Microscopy (disc)			x
Swelling (disc)			x
FTIR (disc)	x	x	x
Tensile (dogbone)	[4]	[4]	
Cyclic loading (dogbone)	[4]	[4]	

Table 1: Testing performed using individual batches in this study and results from [4]

Nomenclature associated with the sample groups used in testing is listed in table 2.

Nomenclature	Sample group
vHDPE	Borsafe HE3490-LS
vHDPEdeg280	vHDPE degraded in air at 280°C
rHDPE	PE-HD-R-E-GREY
uHDPE	Eraclene MP90
uHDPEdeg200	uHDPE degraded in air at 200°C
uHDPEdeg220	uHDPE degraded in air at 220°C
uHDPEdeg240	uHDPE degraded in air at 240°C
uHDPEdeg280	uHDPE degraded in air at 280°C

Table 2: Nomenclature of sample groups used in testing

3.2 Preparation of discs

Flat discs of uHDPE for swelling tests, DSC, OIT, TGA and microscopy were prepared using a 25mm parallel plate geometry on an AR-G2 rheometer from TA-Instruments.

To prevent malfunction of magnetic bearing as sample contracts during cooling, the axial force control was enabled. This function allows for the upper plate to move slightly during cooling to account for contraction of the sample. Mould release spray was applied to the upper and lower plate to ensure easy release of the disc after cooling.

A small spoonful of pellets was loaded onto the plate and left to melt for 1 minute. The plates were moved to a gap of 750 μm and excess melt was trimmed. The AR-G2 was then set to return to ambient conditions, allowing the material between the plates to cool. Once cooled, the upper plate was lifted and the cooled disc was removed from the lower plate. Each disc was cleaned with ethanol to remove excess mould release spray. The discs were prepared at starting temperatures of 200°C and 220°C to remain as close to the properties of the virgin pellets as possible. The degraded discs were prepared by exposing the melt to free air for 30 minutes at 200°C, 220°C and 240°C. The nomenclature used to reference the sample groups is presented in table 2.

Application of mould release spray introduces a possible source of error in crystallization of the discs, as the surface roughness of the AR-G2 plate geometry is changed, and can therefore result in disrupted crystallization behavior. This step was introduced out of necessity, as the plates of the rheometer were impossible to separate after cooling, without application of the mould release spray.

3.3 TGA

TGA can be used to describe the behavior of a polymer as it degrades by tracking mass change over a set temperature gradient. As temperature increases, volatile components degrade from the sample, leading to a decrease in mass [55].

TGA was performed to see the effects of a previous controlled degradation on the degradation temperature. TGA analysis was performed on a SDT-650 from TA Instruments. The mass of the alumina pans used for testing and references were tared prior to test start. A sample of approximately 5mg was cut from prepared discs of rHDPE, vHDPE and uHDPE and placed in a tared alumina pan alongside an identical reference pan.

TGA test method:

1. Ramp 20°C/min to 600°C in nitrogen
2. Switch gas to air
3. Ramp 20°C/min to 1000°C

3.4 DSC

The properties of a polymer during controlled heating and cooling cycle can be determined using DSC. Amorphous polymers have no melting transition, with chains gradually becoming more mobile above the glass transition temperature. Semi-crystalline polymers exhibit a melting transition as well as a glass transition, as some chains are ordered in a crystalline manner, while the remainder of the polymer is amorphous. The amorphous thermal transitions are typically only visible in semi-crystalline polymers of low crystallinity [51].

The degree of crystallinity of a polymer sample can be determined through analysis of the melting transition [51]. The enthalpy of melting of the tested sample is divided by the enthalpy of melting for a theoretically 100% crystalline sample, as in equation 3. The enthalpy of melting for a 100% crystalline polyethylene is recorded in literature at 293 J/g [9].

$$X_c = \frac{\Delta H_m}{\Delta H_{m,100\%}} \cdot 100\% \tag{3}$$

To characterize the effects of degradation on crystallinity, samples of vHDPE and uHDPE were cut from discs prepared as in section 3.2, where the melt was exposed to air for 30 minutes before performing a controlled cooling. For each test, a flat sample of each material of approximately 5 mg was placed in an aluminium pan a with corresponding lid. An identical reference pan was also prepared.

Method parameters for DSC testing of HDPE:

1. Ramp 10°C/min to 300°C
2. Ramp 5°C/min to 20°C
3. Ramp 10°C/min to 300°C
4. Ramp 5°C/min to 20°C
5. Ramp 10°C/min to 300°C

OIT

Oxidation Induction Time (OIT) can be used to determine a materials resistance toward oxidation at a given temperature. This can indicate how long a material can be held at the processing temperature before significant degradation occurs. Antioxidants are often added to a polymer during the pelletizing process to improve the oxidation properties, such that limited degradation occurs during production of the final product. Exposure to oxidative environments at high temperatures results in production of free radicals in the polymer, which in turn react with oxygen to produce carbonyl compounds, seen as yellow and brown discolorations[51].

A flat sample of approximately 5mg was cut from prepared discs of vHDPE and uHDPE and placed in aluminium pan without a lid. An identical reference pan was prepared simultaneously.

OIT was performed to analyze the oxidation resistance at temperatures used in rheological testing and swelling tests. vHDPE was tested at 200°C and 280°C, corresponding to the temperatures tested using LAOS. In addition, uHDPE was tested at 200°C and 220°C, corresponding to the prepared discs. Testing of OIT at 200°C was based on method parameters described in DS/EN ISO 11357-6:2018 [25]

Method parameters for OIT testing of HDPE samples:

1. Equilibrate at 50°C
2. Ramp 10°C/min to 200°C, 220°C or 280°C
3. Isothermal for 5 minutes
4. Switch gas to air
5. Isothermal for 120 minutes

3.5 Rheology

Rheological testing was performed on an AR-G2 rheometer from TA-instruments with a 25mm stainless steel parallel plate geometry. A gap size of 750μm and testing temperature of 200°C were chosen for rheological tests on vHDPE and rHDPE. A small spoonful of pellets was loaded onto the plate and left to melt for 3 minutes before approaching the trim gap of 785μm. The excess material was trimmed from the sides of the plates, and the upper plate was lowered to the set geometry gap of 750μm before starting the test.

The effects of degradation of vHDPE were tested by exposing the melt to free air at 280°C for 30 minutes, whereafter the temperature was lowered to the testing temperature of 200°C and testing proceeded according to the same conditions as for non-degraded samples.

Frequency sweeps were performed at 1% strain amplitude from 100 Hz to 0,1 Hz.

Preliminary frequency sweeps were performed in order to set the optimal testing temperature and gap size, as described in Appendix A.2.

LAOS

Data acquisition for amplitude sweeps was set to transient data instead of correlation data in order to collect stress-strain waveforms for all tested amplitudes. Thus, Lissajous-Bowditch plots were generated for each measured datapoint. The test was set to run from 1% strain amplitude to 400% strain amplitude, with 10 data points recorded per decade. Thus, data was collected from approximately 1,25% oscillation strain to 316% oscillation strain. Amplitude sweeps were performed at frequency of 2Hz and frequency of 8Hz.

In order to find the crossing of G' and G" in the amplitude sweeps, tests must be run at frequencies where G' is above G" in the initial test phase. The crossover can be shifted to lower frequencies for HDPE by lowering the temperature, as elastic behavior is dominant at lower temperatures. However, at lower temperatures, the viscosity also increases, increasing the time needed to achieve the set gap size. Thus, a compromise between temperature and frequency was chosen to avoid additional degradation during the test preparation. Additionally, at high frequencies, initial tests tended to become unstable, with ejection of the sample from the edges of the plates. As a result, the frequencies chosen, 2Hz and 8Hz, reflect upper and lower boundaries of test stability and repeatable test preparation.

3.6 Swelling

Preliminary tests conducted in the RHQI project #9091-00010B at Aalborg University indicated possible effects of solvent interaction in the mechanical failure of HDPE. These results are not yet published. As a result, the diffusion of solvent into an unstressed sample was relevant to characterize, in order to see possible changes to diffusion behavior caused by degradation. Discs of virgin uHDPE prepared at 200°C, and 220°C as well as degraded discs of uHDPEdeg220 and uHDPEdeg240 were tested in Arkopal and xylene at room temperature for 100 hours. Samples were weighed approximately every 1,5 hours for the first 9 hours, then left overnight and checked periodically for 100 hours.

Thuy et al. [64] used a standard surfactant solution of 2% aqueous Arkopal in testing of ESC of HDPE, which was found to accelerate failure compared to distilled water. In addition to its use as a crop protection product, Arkopal is often used in the determination of resistance to ESC of polyethylene[64]. Comparisons of solubility of HDPE in xylene, benzene and toluene in [37], revealed xylene to have the greatest effect on HDPE. Cuadri and Martín-Alfonso [19] performed solubility tests on degraded HDPE in xylene, observing an insoluble fraction for degraded samples, which they attributed to degradation products caused by branching and crosslinking.

Samples were submerged in approximately 5 ml of solvent in a small beaker. Each beaker was covered with parafilm to minimize evaporation.

To minimize contamination of measuring equipment, the sample were patted dry to remove excess solvent, then rinsed in distilled water and patted dry once again. The mass and thickness of each sample was recorded, and the sample was returned to the beaker and covered with parafilm. Evaporation of solvent from sample surface during measurement could cause irregularities in the recorded mass. This source of error was minimized by removing and measuring the samples one at a time in the same order, ensuring identical treatments of all samples.

3.7 FTIR

In order to characterize possible degradation products, ATR-FTIR was performed using a Nicolet iS20 FTIR Spectrometer from Thermo Scientific on the flat discs prepared. The collected FTIR spectra were in the range of 4000-650 cm^{-1} with a resolution of $4cm^{-1}$. 32 scans were collected for each spectrum. The analysis of the FTIR spectrum was performed using SpectraGryph, and focused on the absorbance peak placements.

3.8 Optical Microscopy and SEM

In order to see the structure of the HDPE samples, it was necessary to etch the prepared discs prior to microscopy of the HDPE samples. Molnár et al. [48] improved the visibility of the crystalline structure in HDPE with a selective dissolution of the amorphous layer using hot xylene. As such, a similar method was applied to etch HDPE discs in this study.

A beaker filled with xylene was heated to 130 °C, with glass beads at the bottom to prevent bubbling. The HDPE discs were submerged in the hot xylene for 10 seconds before being removed. Immediately after removal the samples were rinsed thoroughly with ethanol, followed by rinsing in distilled water. Samples were patted dry to remove excess water from the surface, then allowed to briefly air dry.

SEM was performed using a Zeiss EVO LS15 Scanning Electron Microscope with a VPSE G3 Variable Pressure SE detector to improve scanning speeds. Specimens were mounted with double sided tape one at a time. Optical microscopy was performed on a Zeiss Axio Imager.M2m microscope, with 50x magnification.

4 Results and Discussion

The following chapter presents a discussion of the results, where the different test results will be compared, in order to reach a conclusion on the structure-property relations for rHDPE at large deformations and the effect on crystallization.

4.1 Discs

Significant yellowing was evident in preparation of degraded discs, shown in figure 9. The yellowing appeared to be concentrated on the surface of the melt exposed to air for 30 minutes. This was seen by cracks in the yellowed surface on the finished disc, due to the compression of the melt after degradation. Similar results were seen by [69], where recycling of HDPE resulted in yellow and grey coloring compared to virgin HDPE. The color change in [69], analyzed through solar spectral reflectance, was more prominent for blow-molded HDPE bottles with a higher percentage of recycled content. The discs prepared were used for TGA, OIT, DSC, swelling, FT-IR, optical microscopy and SEM.

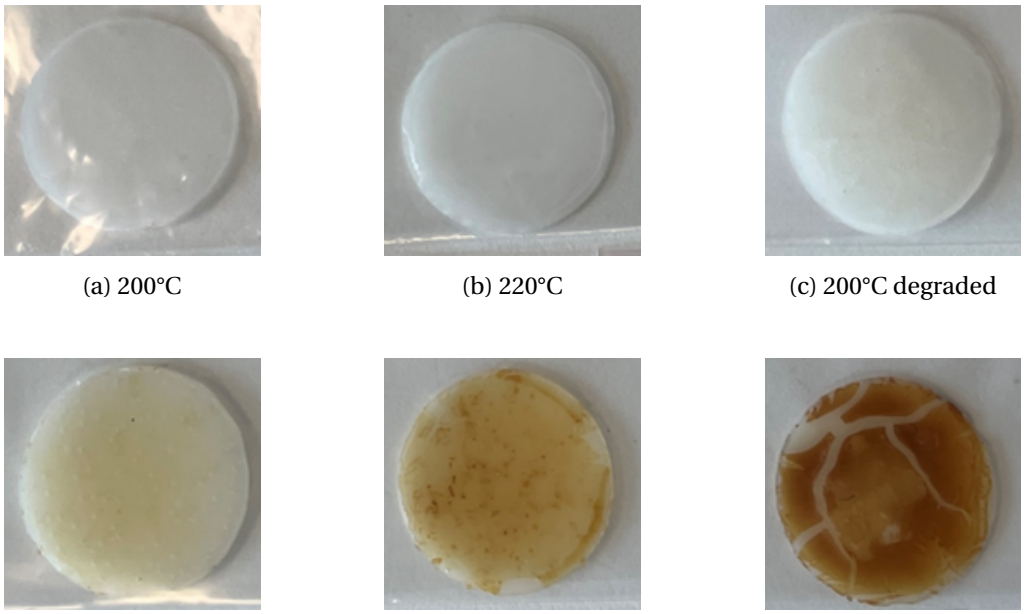

(a) 200°C (b) 220°C (c) 200°C degraded

(d) 220°C degraded (e) 240°C degraded (f) 280°C degraded

Figure 9: Discs of uHDPE prepared at 200°C, 220°C, 240°C and 280°C

4.2 TGA

The degradation temperature used for analysis of TGA results was determined as the inflection point at the rate of maximum degradation as in [19]. TGA performed on vHDPE, vHDPEdeg280 and rHDPE, showed little differences in degradation temperature between vHDPE and vHDPEdeg280, as seen in table 3 and figure 10. The degradation temperature of rHDPE was slightly higher compared to vHDPE.

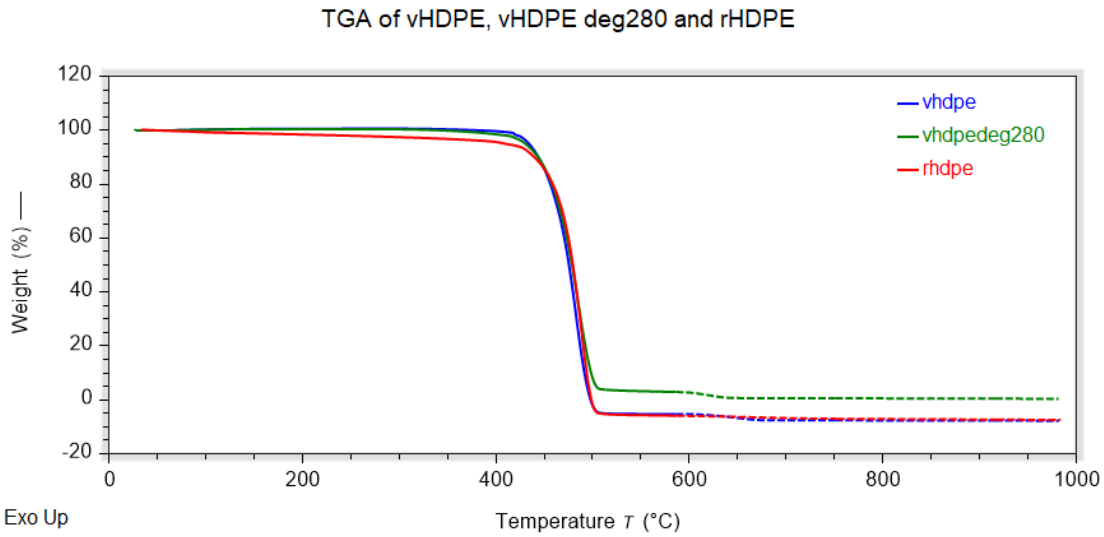

Figure 10: TGA of vHDPE, vHDPEdeg280 and rHDPE

	Degradation temperature [°C]
vHDPE	456,82
vHDPE deg280	456,16
rHDPE	465,13

Table 3: Degradation temperature from TGA of vHDPE, vHDPEdeg280 and rHDPE

TGA of uHDPE, uHDPEdeg220 and uHDPEdeg240 showed increasing degradation temperatures for uHDPEdeg220 and uHDPEdeg240, seen in table 4 and figure 11. Crosslinking during degradation could result in a stronger network, which decomposes at higher temperatures, representing a possible explanation for the behavior seen in the tested samples.

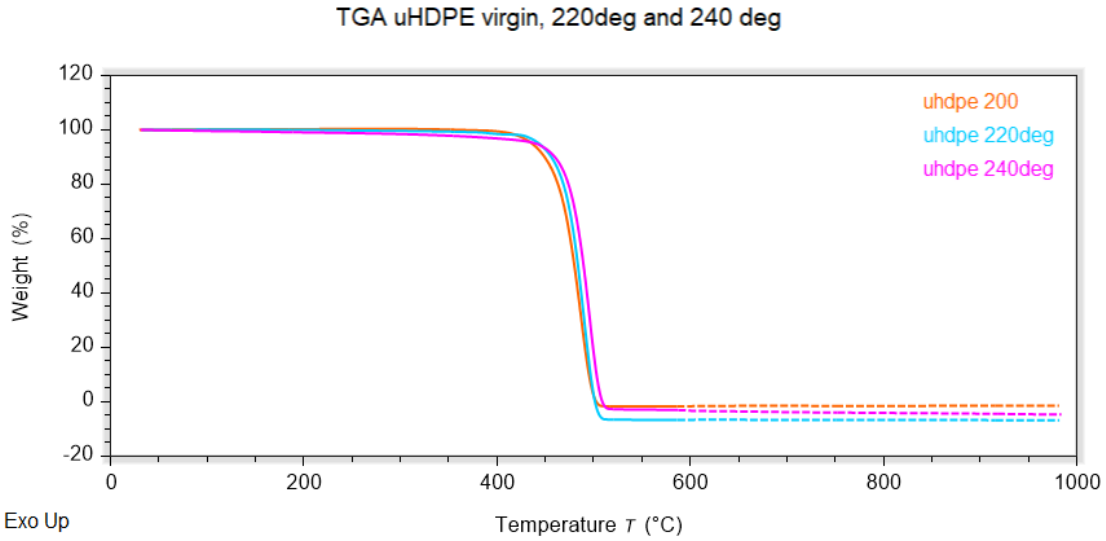

Figure 11: TGA of uHDPE, uHDPEdeg220 and uHDPEdeg240

	Degradation temperature [°C]
uHDPE	463,9
uHDPE 220deg	468,4
uHDPE 240deg	474,9

Table 4: Degradation temperature from TGA of uHDPE, uHDPEdeg220 and uHDPEdeg240

Cuadri and Martín-Alfonso [19] observed shifts of the degradation temperature measured by TGA of HDPE affected by thermo-oxidative degradation to lower temperatures as a result of longer degradation times.

Possible sources of error in TGA testing of uHDPE, vHDPE and rHDPE can be seen by the final weight % of several tested samples. The final weight % of some samples lies below 0%, indicating possible calibration issues. As the amount of residue at the end of the test was not analysed, this source of error was not acted upon. The repeatability of TGA samples is shown in appendix A.4.

4.3 DSC

The degree of crystallinity, X_c, calculated using the enthalpy of melting, ΔH_m, was the main focus of DSC testing of vHPDE, rHDPE and uHDPE. The degradation temperature was increased for uHDPE discs, the degree of crystallinity decreased, corresponding to the decrease in crystallinity between vHDPE and vHDPEdeg. The peak melting temperature, T_m, decreased slightly as well.

For both vHDPE and uHDPE, a decrease in the degree of crystallinity was evident in DSC of degraded samples. An analysis of the effect of degradation temperature on the crystallization behavior was performed for uHDPE, yielding clear degradation effects for samples degraded at 240°C and 280°C, with only minimal differences between the non-degraded sample, uHDPE, and the sample held in air at 220°C, deg220.

Table 5 and figure 12 show the results achieved from the 2nd heating and cooling cycles of vHDPE, vHDPEdeg280 and rHDPE. rHDPE had a higher melting peak, accompanied by a higher degree of crystallinity, compared to vHDPE.

	ΔH_m [J/g]	X_c [%]	T_m [°C]	T_c [°C]
vHDPE	179,8	61,3	129,1	117,6
vHDPE deg280	164,6	56,2	128,6	117,4
rHDPE	195,2	66,6	130,9	120,5

Table 5: Degree of crystallinity of vHDPE, vHDPEdeg280, and rHDPE

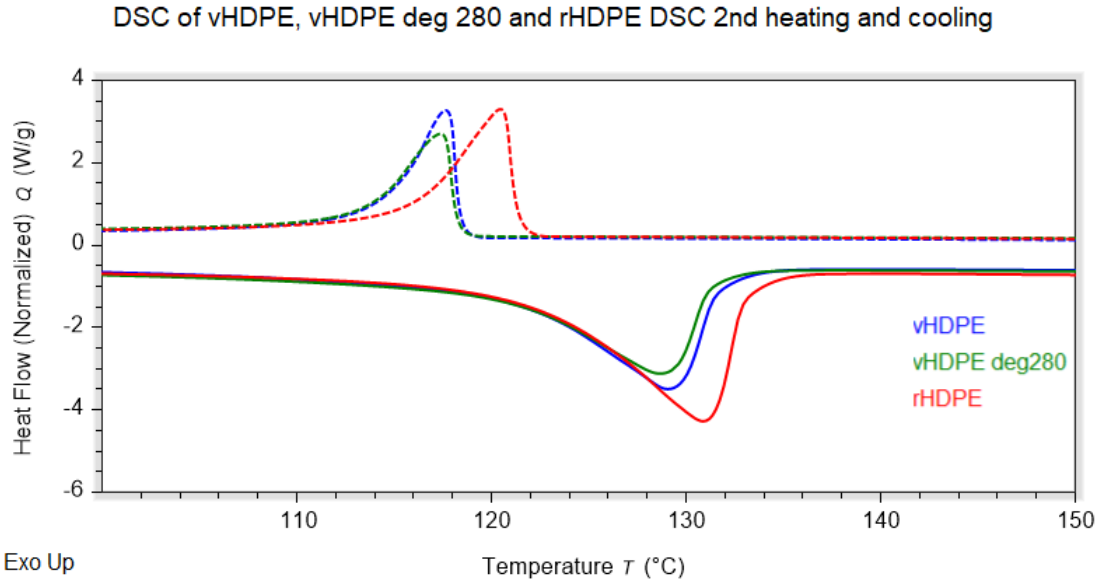

Figure 12: DSC of vHDPE, vHDPEdeg280, and rHDPE

Table 6 and figure 13 show the results achieved from the 2nd heating and cooling cycles of uHDPE,

uHDPEdeg220, uHDPEdeg240 and uHDPEdeg280. The greatest effects of thermo-oxidation were seen for the thermogram of uHDPEdeg280, which has a clear shift in the melting peak, as well as a decrease in the calculated degree of crystallinity.

	Δh_m [J/g]	X_c [%]	T_m [°C]	T_c [°C]
uHDPE	229,51	78,3	132,65	119,99
uHDPEdeg220	226,60	77,3	132,26	120,24
uHDPEdeg240	208,34	71,1	132,33	119,98
uHDPEdeg280	201,23	68,7	131,24	119,61

Table 6: Degree of crystallinity of uHDPE, uHDPEdeg220, uHDPEdeg240 and uHDPEdeg280

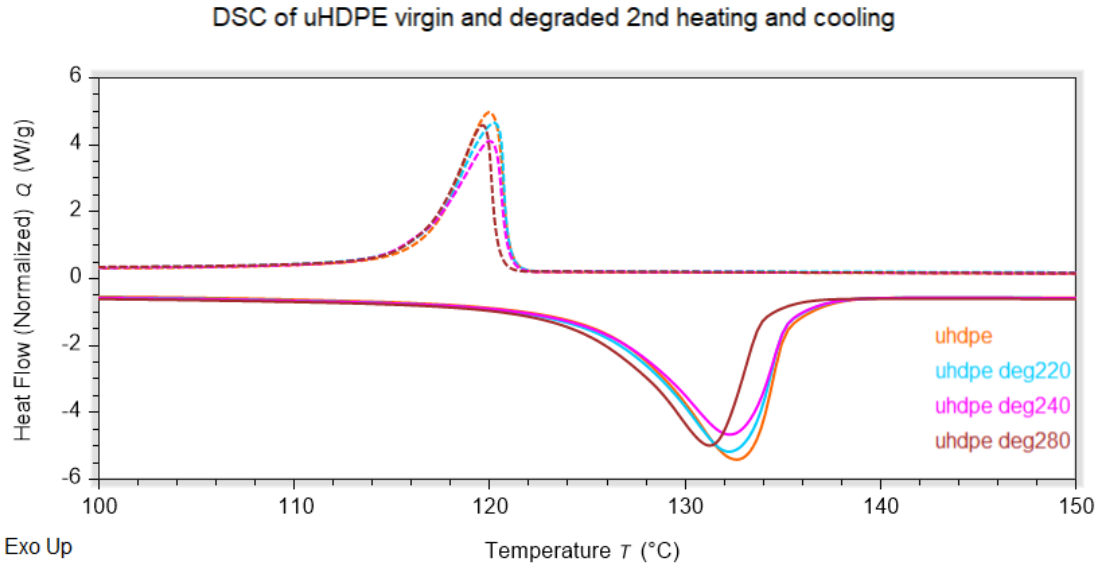

Figure 13: DSC of uHDPE, uHDPEdeg220, uHDPEdeg240, uHDPEdeg280

A decrease in the degree of crystallinity from DSC, along with the increase in degradation temperature observed from TGA, suggests crosslinking during degradation, as crosslinks hinder crystal growth and create physical links in the polymer.

Decreases in the degree of crystallinity of HDPE as a result of degradation and reprocessing were observed in [15, 45, 52, 67, 69]. Zeng et al. [69] saw a decrease in crystal size and degree of crystallinity as a result of mechanical recycling of HDPE. This was attributed to contaminants introduced during the recycling process, which hindered the formation and growth of crystals.

In contrast, [30, 61] observed increases in the degree of crystallinity of HDPE as a result of thermo-oxidative ageing. This was attributed to a reduction in the molecular weight, which enabled easier crystallization. Accelerated ageing of HDPE in [30] led to a broadening of the melting peak in DSC, attributed to changes in molecular weight and changes in the size of crystallites. Zattera et al. [68] observed increases in the degree of crystallinity as a result of initial

recycling of HDPE, which was associated with chain scission, with a change in the dominant degradation mechanism toward crosslinking as the number of reprocessing cycles increased.

The explanation behind the discrepancies in the behavior of the degree of crystallinity of HDPE as a result of reprocessing, can possibly be found in the complexity of the underlying degradation mechanisms. This complexity was seen by Cuadri and Martín-Alfonso [19] where decreases in crystallinity of HDPE melts degraded in air were recorded, which were hypothesized to be the result of the formation of degradation products and possible chain branching, leading to changes to the microstructure. Similarly, [45] hypothesized that a crosslinked network was formed during reprocessing cycles, which limited the organization of chains into larger crystal domains. Dominance of chain scission in the degradation of HDPE was prevalent in nitrogen atmospheres in [19], where the degree of crystallinity subsequently increased.

OIT

OIT was performed to confirm the presence of degradation at the temperature used for vHDPEdeg280 in rheological testing, as well as comparing the oxidation resistance of vHDPE and uHDPE. Alzerreca et al. [3] performed OIT on virgin and recycled HDPE pipe material, observing decreased oxidation times for recycled HDPE compared to virgin HDPE.

	vHDPE [min]	uHDPE [min]
200°C	N/A	6,3
220°C	85,8	1,89
280°C	0,44	not tested

Table 7: OIT of vHDPE and uHDPE

No OIT was present within 120 minutes of oxidation for vHDPE at 200°C. Subsequent OIT tests were performed for vHDPE at 280 °C, yielding an oxidation time of 0,44 minutes, or approximately 26 seconds. Thus, at 280°C, the rapid oxidation should result in a clear change in properties from vHDPE. These results support the degradation temperature used for rheological testing of vHDPEdeg. The OIT test of uHDPE at 200°C is shown in figure 14, focused on the scan after the gas was changed to air. OIT scans of the remaining samples are shown in appendix A.1.

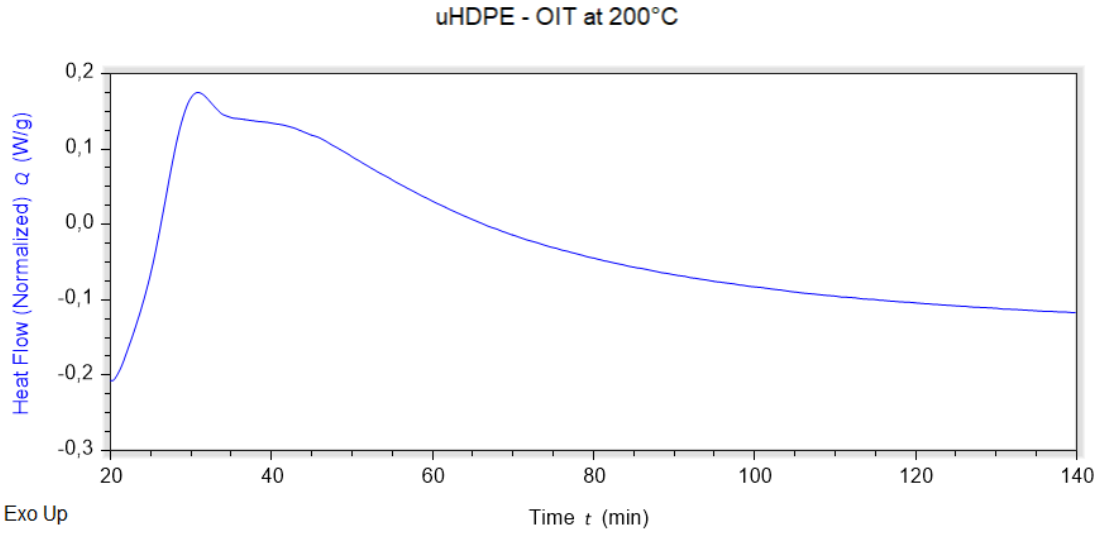

Figure 14: Step 5 of OIT of uHDPE at 200°C

The OIT results of vHDPE and uHDPE show significantly faster oxidation times for uHDPE, with uHDPE oxidizing within approximately 6,3 minutes of exposure at 200°C. When the testing temperature is increased to 220°C, vHDPE had an OIT of 5,8 minutes, where uHDPE had an OIT of 1,9 minutes. As oxidation occured rapidly at 220°C for uHDPE, the test was not performed at 280°C. The prevalence of carbon black in vHDPE provides a possible explanation for the higher oxidation resistance compared to uHDPE [54].

4.4 Rheology

Reprocessing of HDPE by twin-screw extrusion in [41] indicated an increase in MW and MWD, tested by SAOS rheology. As a result, Kealy [41] concluded the mechanisms of degradation of HDPE during mechanical recycling to be primarily competition between chain scission and side chain branching. Zeng et al. [70] also found increased chain irregularity for recycled HDPE due to competing degradation mechanisms, resulting in a broader MWD.

Thermal oxidation of polyethylene in [34, 35] yielded an increase in side chain branching, as well as an increase in low MW products. The crystalline content was simultaneously found to decrease as a function of oxidation time. Initial degradation resulted in a decrease in MW, attributed to chain scission. However, their results showed that as oxidation time and temperature were increased, side chain branching and crosslinking increased the MW and MWD of recycled HDPE.

Frequency sweeps

Comparison of frequency sweeps of vHDPE to vHDPEdeg280 and rHDPE yield contrasting results for vHDPEdeg and rHDPE. The crossover point of G' and G" shifts right, with no vertical change for rHDPE, indicating a lower MW and no change in the MWD. As rHDPE is a PCR bottle grade HDPE, the MW is difficult to compare accurately to vHDPE, as the HDPE grades used in processing of rHDPE could have lower initial MW compared to vHDPE. As a result it is more representative to compare the MW and MWD of vHDPE to vHDPEdeg280. In this case, changes to both are expected to stem from the degradation mechanisms active during exposure of the melt to air.

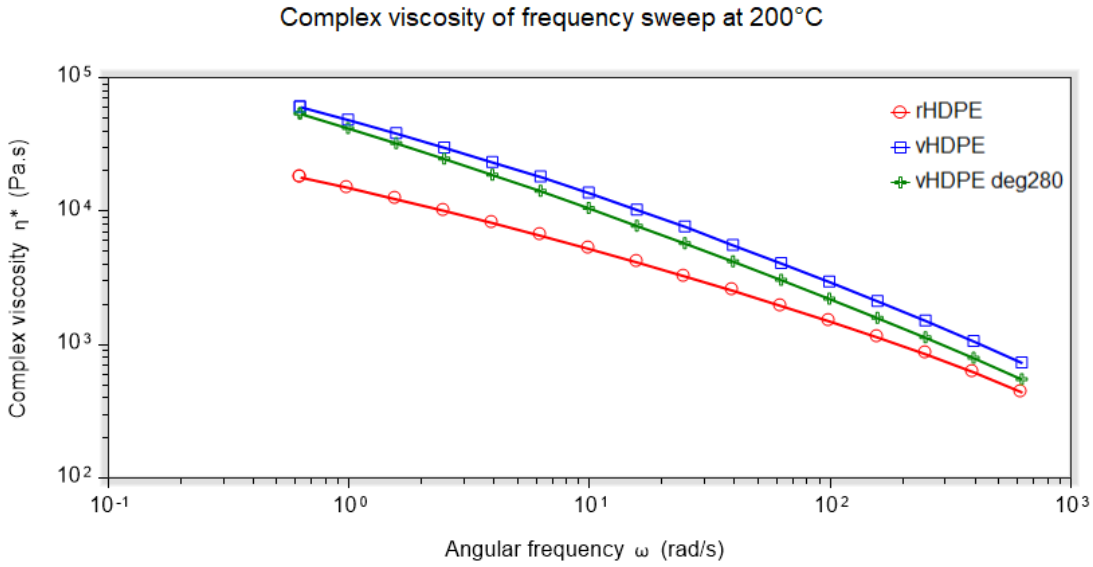

Figure 15: Complex viscosity of frequency sweeps of vHDPE, vHDPEdeg280 and rHDPE at 200°C

The crossover point of vHDPEdeg280 is not visible at the tested frequencies. However, the trends of G' and G" indicate a shift left and slightly down, signifying an increase in MW along with a

broader MWD. This increase in MW contrasts with expectations from the complex viscosity in figure 15, where the viscosity of vHDPEdeg280 is lower than vHDPE. Increases in MW typically align with increases in viscosity [1]. A possible explanation of this is the broadened MWD of vHDPEdeg280. A broader MWD in combination with higher MW indicates that the fraction of high MW chains has increased, as well as the fraction of low MW chains. Low MW chains have the potential to act as lubrication of higher MW chains, hindering the natural entanglement of high MW chains [50].

	Frequency [Hz]	modulus [MPa]
vHDPE	0,194781	0,037527
vHDPEdeg280	-	-
rHDPE	1,66818	0,037616

Table 8: Crossover point of G' and G" in frequency sweeps of vHDPE, vHDPEdeg280 and rHDPE

Figures 16, 17 and 18 show the frequency sweeps of vHDPE, vHDPEdeg280 and rHDPE performed at 200°C.

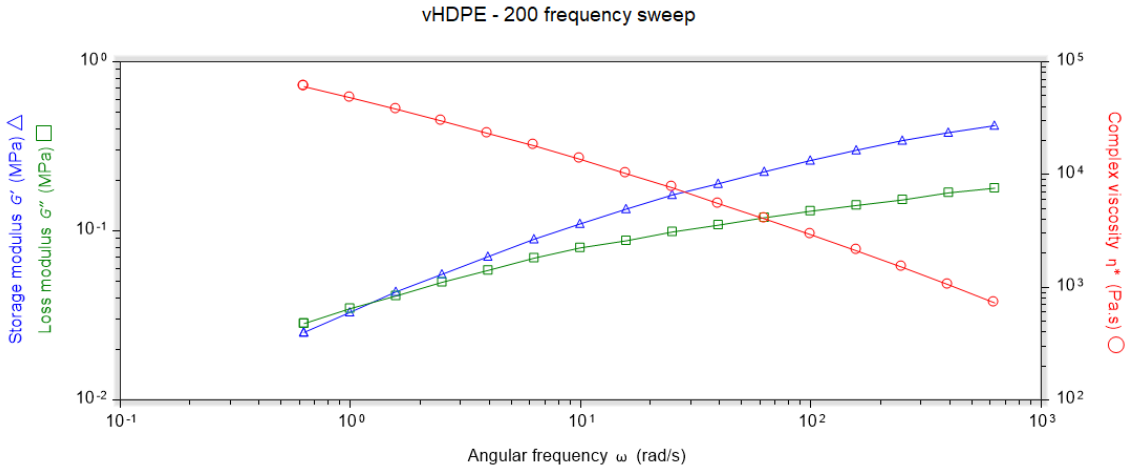

Figure 16: Frequency sweep of vHDPE at 200°C

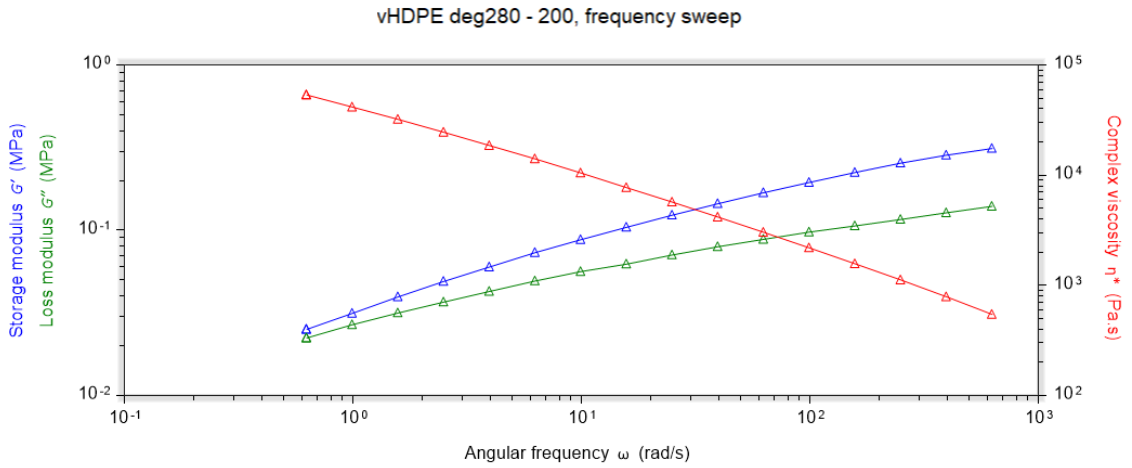

Figure 17: Frequency sweep of vHDPEdeg280 at 200°C

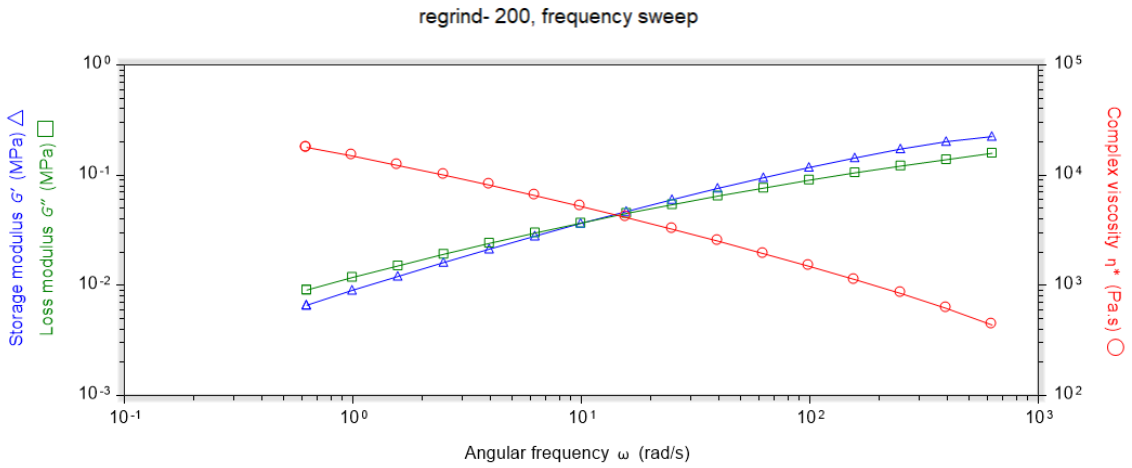

Figure 18: Frequency sweep of rHDPE at 200°C

The results of frequency sweeps of vHDPE, rHDPE and vHDPEdeg280 show changes to the crossover points of G' and G", indicating increases of MW and broadening of the MWD for vHDPEdeg280, and decreased MW for rHDPE.

LAOS

As the internal polymer structure is less flexible at higher frequencies, amplitude sweeps performed at a high frequency were expected to show higher values of G' and G" compared to those performed at a low frequency. Additionally, a steeper decrease of the storage modulus after the LVE region can be indicative of an internal macromolecular configuration controlled by more brittle behavior [47].

The authors of [42] studied relations between microscopic rearrangements and rheological flow behavior with LAOS. Their research focused on non-linear structure-rheology relationships under dynamic shearing, relationship between behavior in amplitude sweep and non-linearity

in Lissajous-Bowditch plots for a polymer-micellar solution. The aim of their research was to provide framework for the study of complexity of structure-rheology relations of polymers and other soft materials under high deformation conditions.

	2Hz strain [%]	**8Hz** strain [%]
vHDPE	25	20
vHDPEdeg280	31	24
rHDPE	50	45

Table 9: Yield points - onset of non-linearity of G' from amplitude sweeps

The yield points of amplitude sweeps of vHDPE, vHDPEdeg280 and rHDPE are listed in table 9. The onset of non-linearity is defined here as a 5% change in G'. The values listed are approximate values based on the data points from amplitude sweeps. From this, it is clear that rHDPE has the highest yield point at both test frequencies, followed by vHDPEdeg280 and vHDPE. The difference in strain of the yield point is approximately 5% lower at a test frequency of 8Hz for all samples compared to a test frequency of 2 Hz. This aligns with the expectation that higher frequencies correspond to more brittle behavior of the internal structure.

	2 Hz		**8 Hz**	
	strain [%]	modulus [MPa]	strain [%]	modulus [MPa]
vHDPE	187,48	0,032539	237,02	0,026568
vHDPEdeg280	247,99	0,023798	180,83	0,025039
rHDPE	31,42	0,036637	101,04	0,04304

Table 10: Amplitude sweep crossover points for vHDPE, vHDPEdeg280 and rHDPE at 2Hz frequency and 8Hz frequency

The crossover points of G' and G" in amplitude sweeps constitute the flow point in the test, and are listed for the tested materials in table 9. For both tested frequencies, rHDPE reaches the flow point first. This corresponds to the behavior observed for HDPE in the frequency sweep, as the loss modulus is dominant at higher frequencies than for vHDPE and vHDPEdeg.

Lissajous-Bowditch plots can be used to visualise non-linearity of amplitude sweeps. A steeper decline of G' and G" in the non-linear region correlates to a greater shift from the elliptical shape of the linear region [42]. Figures 19-24 show the amplitude sweeps of vHDPE, vHDPEdeg280 and rHDPE with corresponding Lissajous-Bowditch plots of stress-shear rate.

Figure 19, 20 and 21 show the amplitude sweeps performed at a frequency of 2Hz for vHDPE, vHDPEdeg280 and rHDPE, respectively.

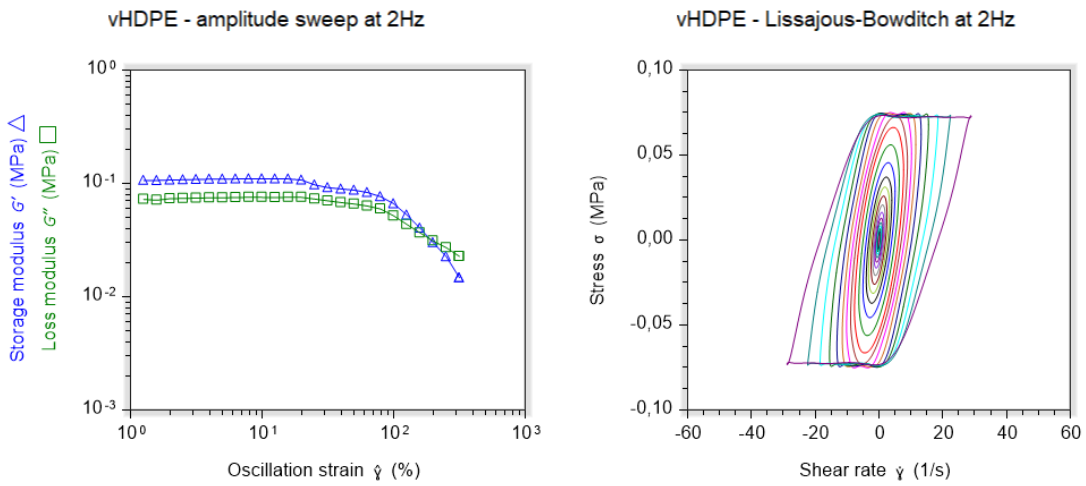

(a) (b)

Figure 19: vHDPE amplitude sweep (a) and Lissajous-Bowditch representation (b)

For vHDPE and vHDPEdeg280, a clear shift from the ellipsoidal shape of the LVE region is seen in the Lissajous-Bowditch plots in figure 19b and 20b, with the shape becoming more organic as the shear rate increases. This corresponds to the decline of G' and G" outside of the LVE region.

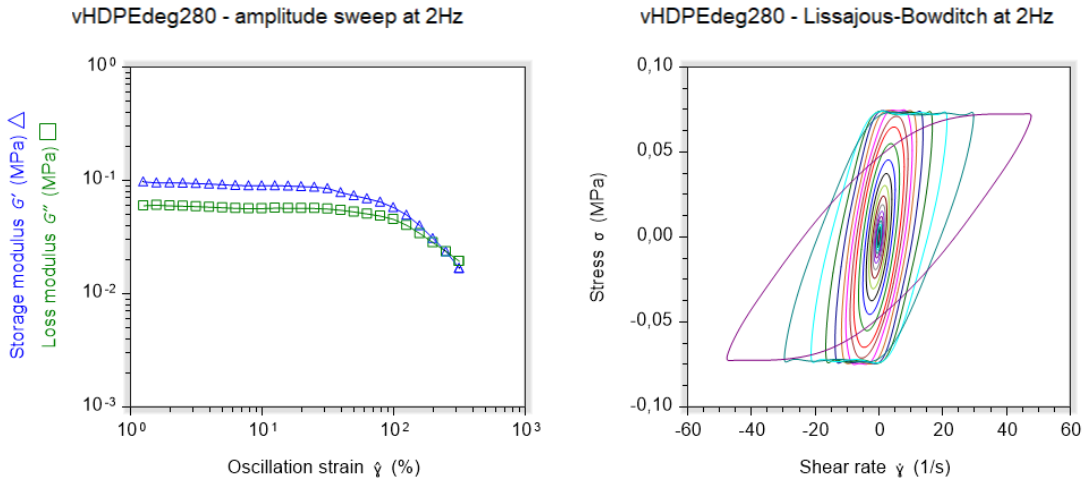

(a) (b)

Figure 20: vHDPEdeg280 amplitude sweep (a) and Lissajous-Bowditch representation (b)

In contrast to vHDPE and vHDPEdeg280, for rHDPE, the shape of the stress-shear rate curves in figure 21b remain ellipsoidal through the entire test, despite a clear departure from the LVE region in the amplitude sweep in figure 21a.

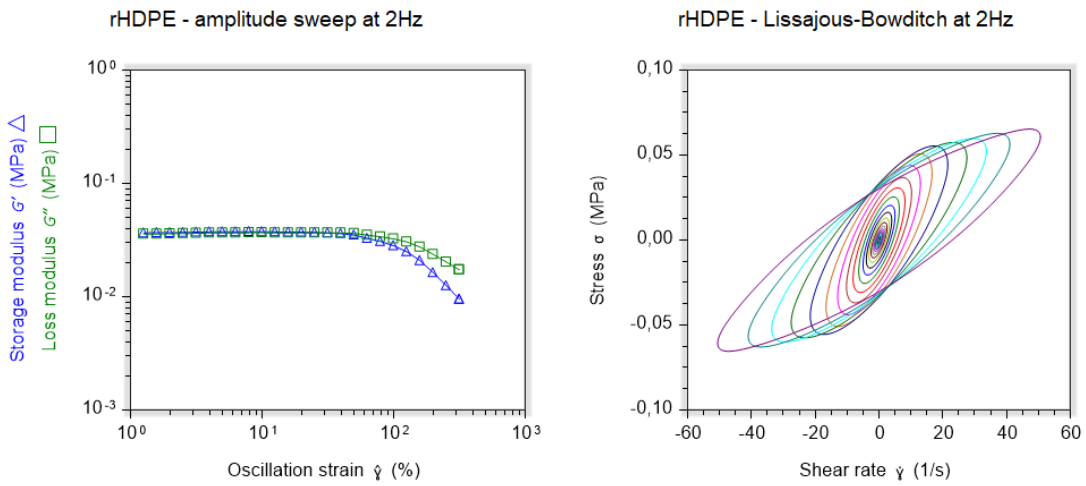

(a) (b)

Figure 21: rHDPE amplitude sweep (a) and Lissajous-Bowditch representation (b)

Figure 22, 23 and 24 show the amplitude sweeps performed at a frequency of 8Hz for vHDPE, vHDPEdeg280 and rHDPE, respectively.

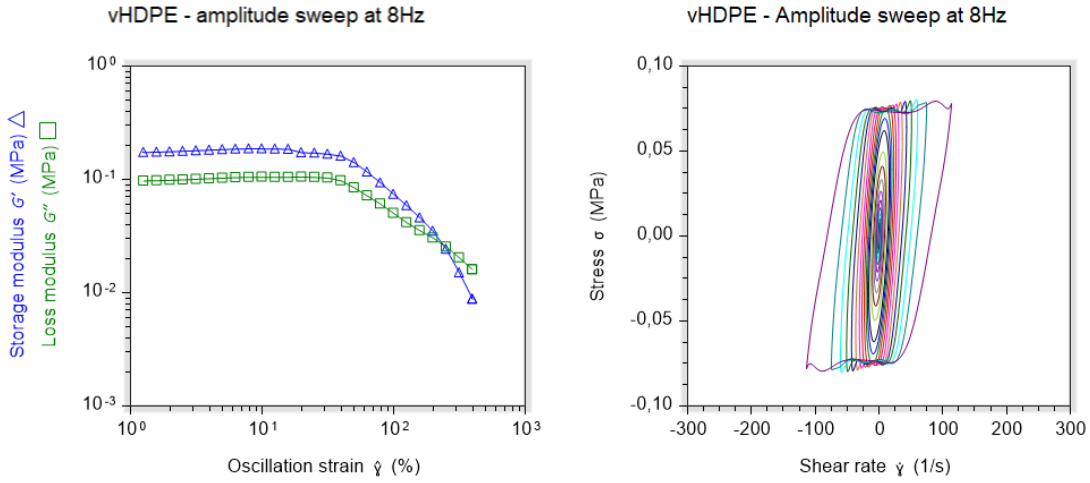

(a) (b)

Figure 22: vHDPE amplitude sweep (a) and Lissajous-Bowditch representation (b)

The amplitude sweep of vHDPEdeg280 in figure 23a remains in the LVE region at higher strain amplitudes compared to the amplitude of vHDPE in figure 22a. This is accompanied by a steeper decline of G' and G" for vHDPEdeg280, which can be clearly seen by the stress-shear rate plot in figure 23a, which transforms completely from the original ellipsoidal relation.

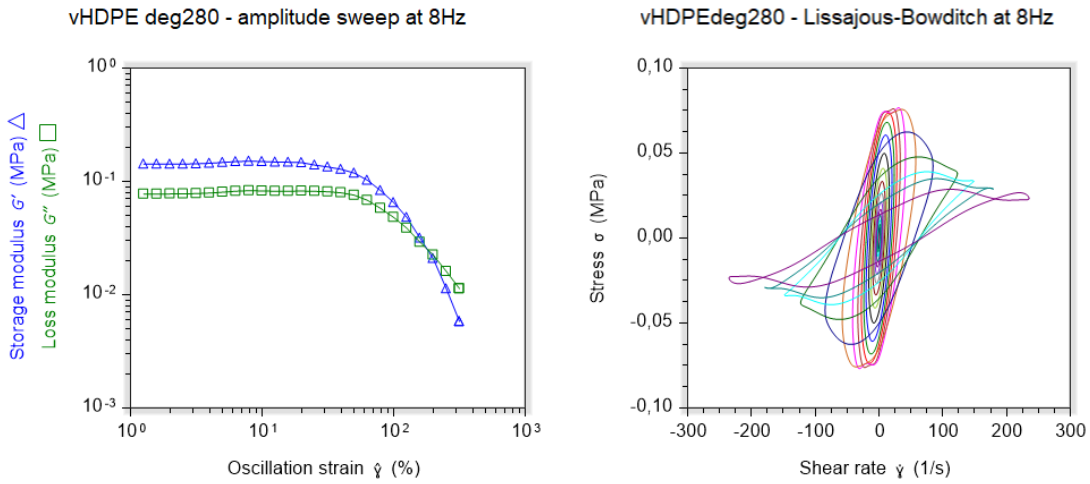

(a) (b)

Figure 23: vHDPEdeg280 amplitude sweep (a) and Lissajous-Bowditch representation (b)

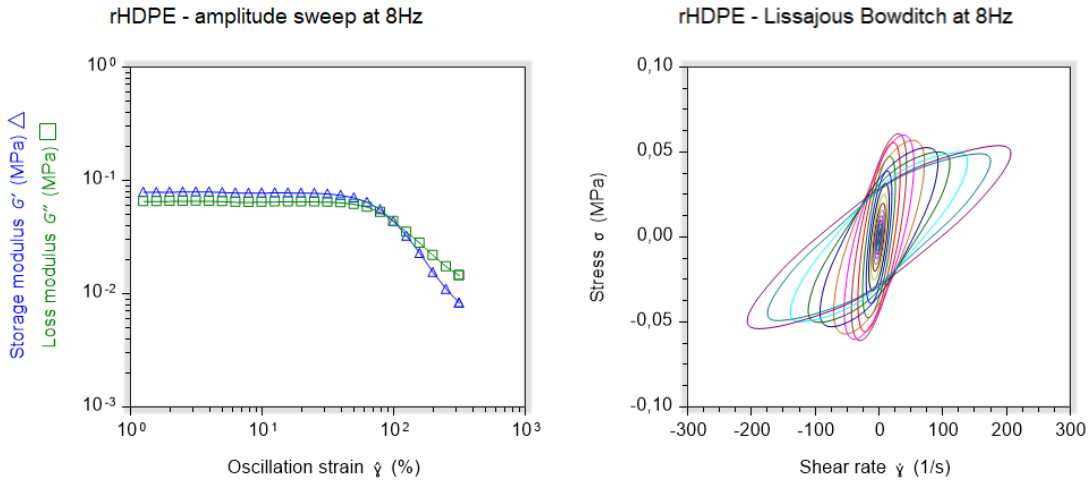

(a) (b)

Figure 24: rHDPE amplitude sweep (a) and Lissajous-Bowditch representation (b)

The effects of the non-linearity in vHDPE and vHDPEdeg280 were exacerbated by LAOS sweeps at higher frequencies, which highlights the frequency dependency of the brittle behavior of the internal structure.

4.5 Swelling

Baddour et al. [6] found that sorption of solvents into HDPE films increased with lower crystallinity. Solubility tests in xylene performed by Cuadri and Martín-Alfonso [19] showed an insoluble fraction, due to chain branching and crosslinking.

The swelling tests in Arkopal showed no significant changes to any samples after 100 hours exposure. This is clear from figure 25, where the mass of all of the tested samples varies slightly between each test checkpoint, with no clear trends. Thus, mass fluctuations observed as a result of testing in Arkopal were attributed to measurement uncertainty.

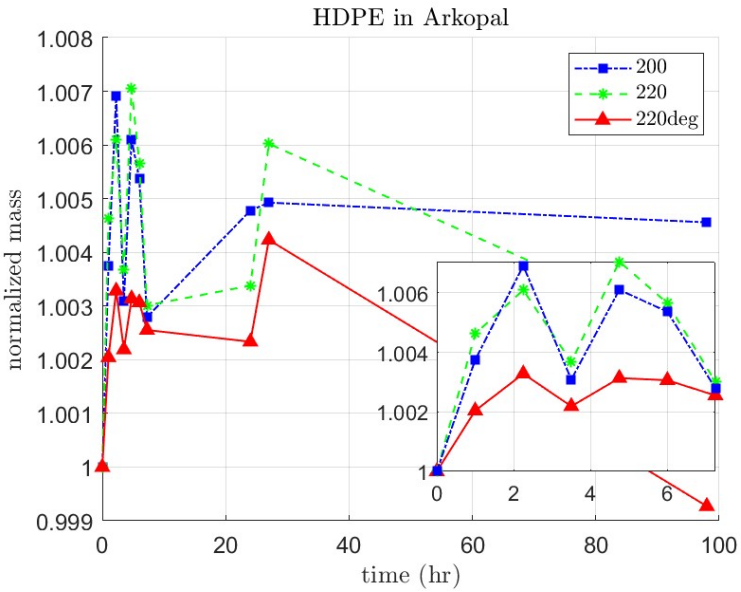

Figure 25: HDPE swelling in Arkopal

Samples submerged in xylene showed clear mass increases at the first checkpoint, with a logarithmic increase in mass until an equilibration of mass, seen in figure 26. Initially only samples of virgin samples of uHDPE produced at 200°C and 220°C, as well as a degraded sample of uHDPE produced at 220°C were tested in xylene, corresponding to the samples tested in Arkopal. Due to little differences observed between the samples, the test was repeated with a degraded uHDPE sample produced at 240°C. The increase in mass of the uHDPE240deg sample occurred more rapidly than all other samples, which aligns with expectations from the degree of crystallinity seen from DSC results. This is due to easier diffusion of solvents through amorphous regions compared to crystalline regions [51].

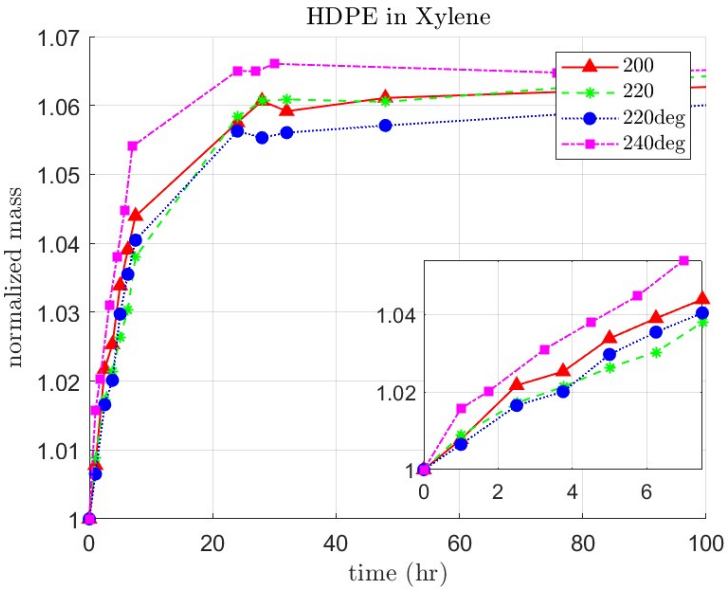

Figure 26: HDPE swelling in xylene

4.6 FTIR

The characteristic peaks of HDPE visible in all of the FTIR spectra are comprised of three strong CH_2 double absorption peaks at 718-729cm^{-1}, 1462-1472cm^{-1} and 2847-2914cm^{-1}. The spectra of vHDPE, rHDPE and uHDPE show only the characteristic peaks. These peaks correspond to the results achieved by [19, 26, 30, 49, 52, 69].

Cuadri and Martín-Alfonso [19] recorded noticeable changes to IR peaks of degraded HDPE, particularly related to absorption peaks of carbonyl groups. Similarly, FTIR analysis of recycled and virgin HDPE in [69] revealed that peaks of carbonyl, ester and hydroxyl groups were more prominent for recycled HDPE compared to virgin HDPE.

FTIR analysis of the vHDPEdeg280 spectrum, seen in figure 27, showed the appearance of an additional peak at 1713 cm^{-1}, corresponding to the placement of peaks of carbonyl groups seen in [19, 26, 30, 69].

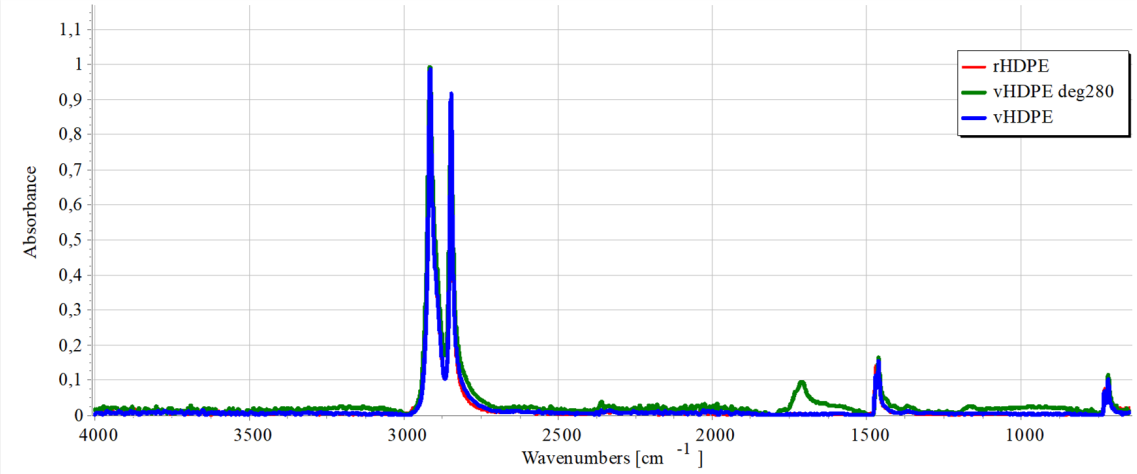

Figure 27: FTIR of vHDPE, vHDPEdeg280 and rHDPE

FTIR of uHDPEdeg220 and uHDPEdeg240, seen in figure 28, showed an additional broad peak at 1150-1250 cm^{-1}, corresponding to the absorption peaks of ester groups associated with oxidation seen in [69]. This peak increased in intensity as the degradation temperature increased from 220°C to 240°C.

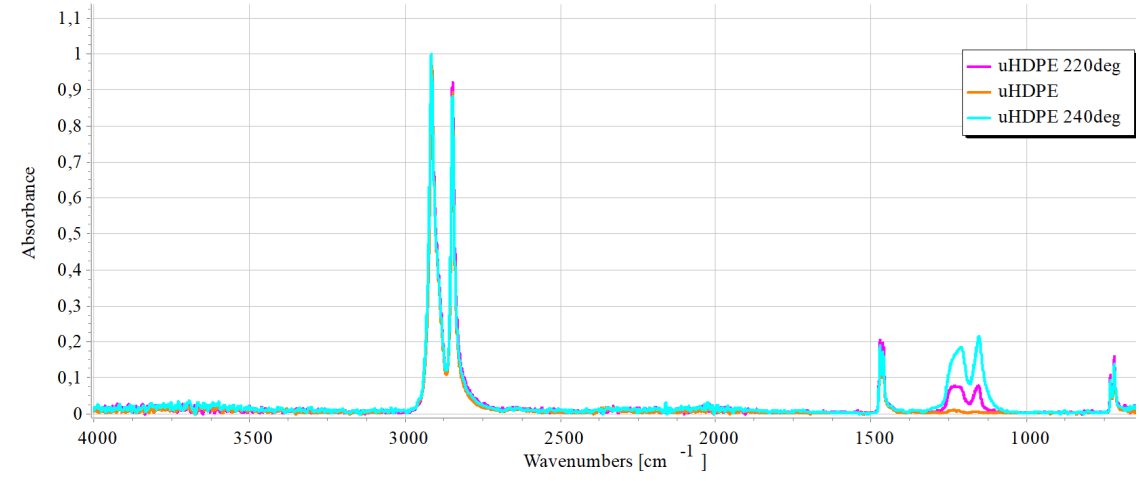

Figure 28: FTIR of uHDPE, uHDPEdeg220 and uHDPEdeg240

Appearance of new absorption peaks of carbonyl and ester groups confirm the presence of oxidation products in the degraded materials. These oxidation products could also contribute as contaminants, effectively limiting crystalline growth.

4.7 Optical microscopy and SEM

Zeng et al. [69] observed morphology changes due to recycling of HDPE. As the recycled content increases, the surface morphology of the HDPE tested by [69] showed a rougher surface with increasing prevalence of pits and cracks. This was attributed to the mechanical recycling process, where prolonged exposure to increased temperatures promotes degradation by crosslinking, leading to irregularities in chain lengths and morphology. Cross-sections of vHDPE and rHDPE bottles analysed using SEM by [69] also showed a higher porosity as recycled content increased, with more fibrous structures.

Due to time and equipment constraints, only virgin uHDPE and uHDPEdeg220 were analysed in SEM and optical microscopy.

Significant whitening of the samples was observed as a result of etching, with the original samples having semi-translucent properties, as shown in figure 9. Any translucency in the original specimens was removed completely as a result of the etching process.

(a) uHDPE etched for 10 seconds

(b) uHDPEdeg220 etched for 10 seconds

(c) uHDPEdeg240 etched for 10 seconds

Figure 29: etched samples

In addition to the whitening observed, the hypothesis relating to the yellowing of discs only appearing on the surface was confirmed by visual inspection of etched samples. The yellowed surface in figure 29b and 29c appears wrinkled compared to the surface of the original samples in figure 9. The etching appeared to lift the yellowed surface slightly, causing further cracks.

(a) uHDPEdeg220 etched for 5 seconds

(b) uHDPE virgin etched for 5 seconds

(c) uHDPE virgin etched for 20 seconds

Figure 30: etched samples

Preliminary testing of the etching time of a virgin uHDPE sample yielded over-etching of the sample at 20 seconds etching time. This was seen by a significant roughening of the surface in figure 30c. Hence, samples of uHDPE and uHDPEdeg220 were etched for only 5 seconds, seen in figure 30b and 30a, maintaining the surface integrity. The etched samples are shown in figure 30 and 29.

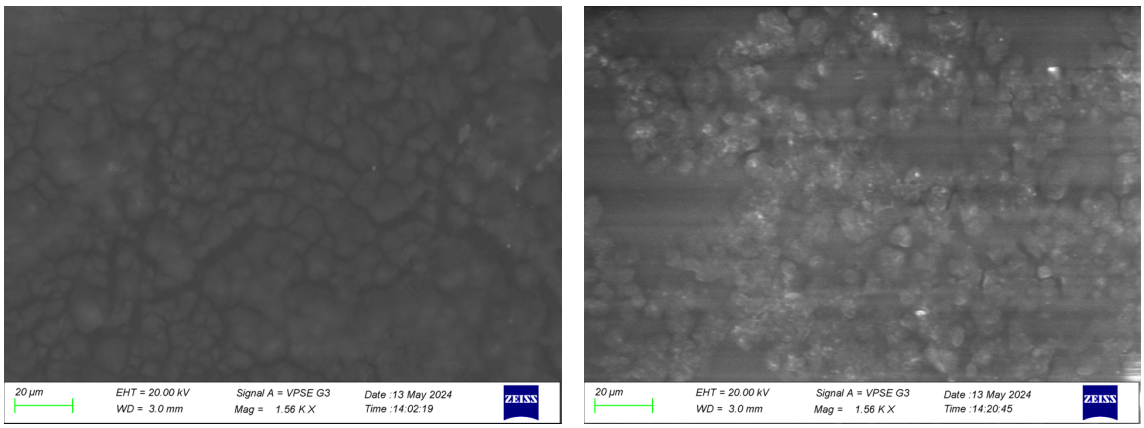

(a) uHDPE disc prepared at 200°C

(b) uHDPE degraded disc prepared at 220°C

Figure 31: SEM of etched samples at 1560x magnification

SEM of a virgin uHDPE disc and a degraded uHDPE disc (uHDPEdeg220), etched in hot xylene for 5 seconds yielded unclear results. As seen in figure 31b, significant noise interrupted the clarity of the images. Achieving proper ratios of brightness and contrast for the tested samples was not possible within the testing time-frame, resulting in fairly dark images where changes in microstructure are difficult to observe. Based on the images obtained, an increased structural irregularity can be seen for the degraded disc compared to the virgin disc.

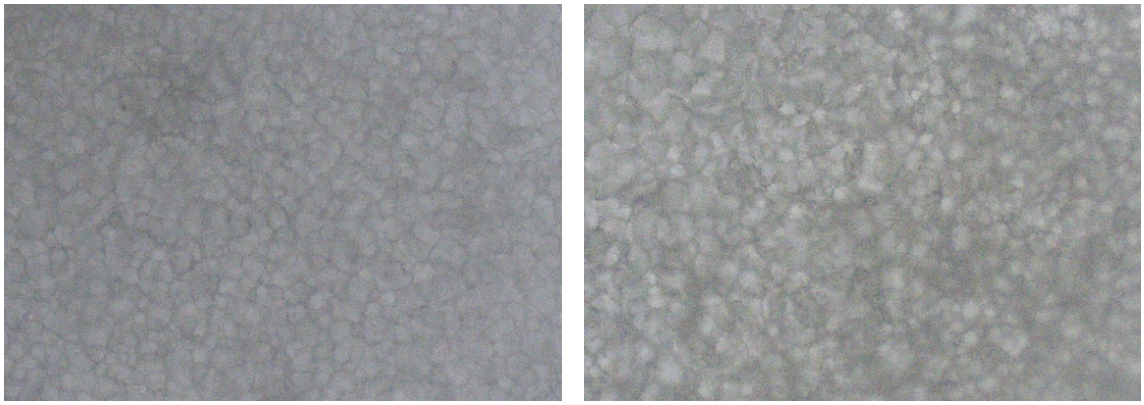

(a) uHDPE disc prepared at 200°C (b) uHDPE degraded disc prepared at 220°C

Figure 32: Optical microscopy of etched samples at 50x magnification

Optical microscopy analysis of the same samples revealed similar structures to those seen in SEM, with increased inhomogeneity of the crystalline structure in the degraded sample compared to the virgin sample. This was seen by an increased roughness of the interfaces between crystalline regions, as well as a greater difference in the sizes of the formed crystal structures.

5 Conclusion and Future Works

The degradation mechanisms of HDPE were found in literature to be a complex combination of chain scission, chain branching and crosslinking. The SCG mechanisms of degraded HDPE were found in literature to be influenced by the degradation mechanisms, leading to complex changes in the crystallinity and molecular structure. The degradation of samples was clear through analysis of TGA, OIT and FTIR, as well as in the increased inhomogeneity of the structure of degraded samples observed using SEM and optical microscopy. DSC of vHDPE and uHDPE, as well as the degraded samples, resulted in a lower degree of crystallinity as the degradation temperature increased, which corresponded to the faster swelling of uHDPEdeg240 in xylene.

The complexity of the degradation behavior was highlighted in rheological frequency sweeps of vHDPE, vHDPEdeg280 and rHDPE. The shift of the crossover point of vHDPEdeg280 indicated higher MW along with a higher MWD, which contrasted with the decrease in complex viscosity. LAOS of vHDPE, vHDPEdeg280 and rHDPE revealed increased non-linearity in Lissajous-Bowditch plots resulting from the degradation of vHDPE. In addition, the steepness of the decline of G' in the amplitude sweep was clearer for vHDPEdeg, correlating to a possible increase in the brittle behavior of the internal structure. Microscopy of uHDPE supported the complexity of degradation, as the degraded sample yielded higher structural inhomogeneity. The results of LAOS tests support the use of the method in tracking the effects of degradation on the structural properties of the polymer network. The effects of degradation on the internal structure of HDPE were investigated through LAOS and crystallinity, with results showing structural changes corresponding to complex degradation mechanisms.

To support the value of LAOS as a tool for investigation of structural behavior, an increased frequency interval is suggested in future investigations. This was not implemented in this thesis, as equipment limitations resulted in a narrow frequency interval to avoid wall-slip and unintended artifacts in testing. Further rheological testing should also be expanded to include the second virgin HDPE tested in this thesis, uHDPE, to ensure continuity in the degradation mechanisms of non-colored HDPE with carbon black filled HDPE. Additionally, x-ray analysis can be utilized as a tool for mapping the crystalline behavior to support results from DSC. Wide- and Small-Angle X-ray Scattering (WAXS and SAXS) can be used to further characterize the crystalline structure in terms of lamellar area and sizes of crystals. Microscopy analysis of a wide range of durations of etching in hot xylene would broaden the understanding of the structural properties of virgin and degraded HDPE. An investigation of etching in moderately heated xylene would provide perspectivation on the possible influence of etching temperatures on the visibility of HDPE structures.

Similar testing on amorphous polymer types, such as polyethylene terephthalate (PET) should be implemented, in order to further catalogue the failure mechanisms of polymer chains during SCG. This would enable a more precise study of the effects of amorphous and crystalline regions on failure.

A Appendix

A.1 DSC and OIT

Full DSC scans

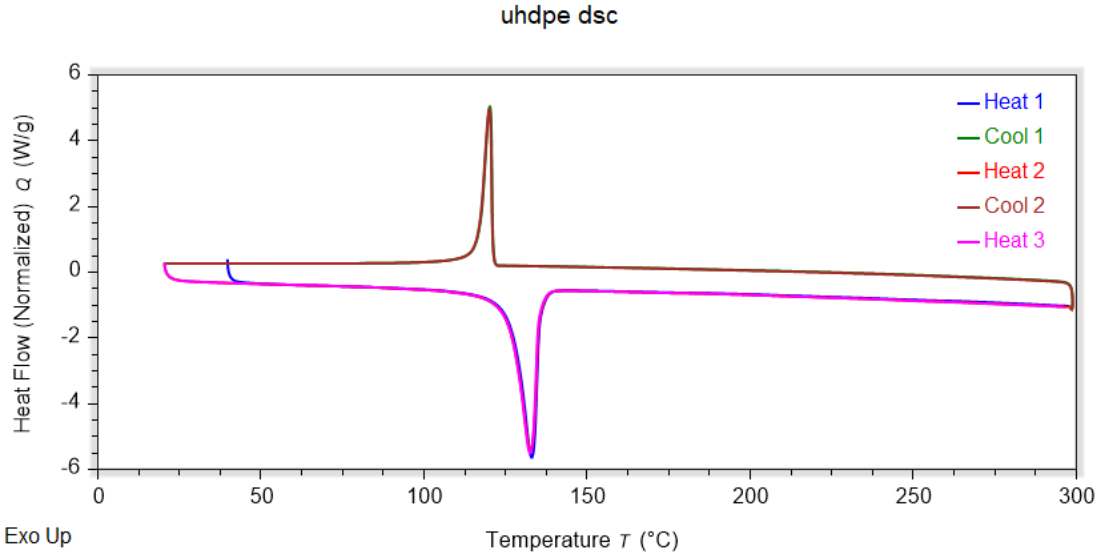

Figure 33

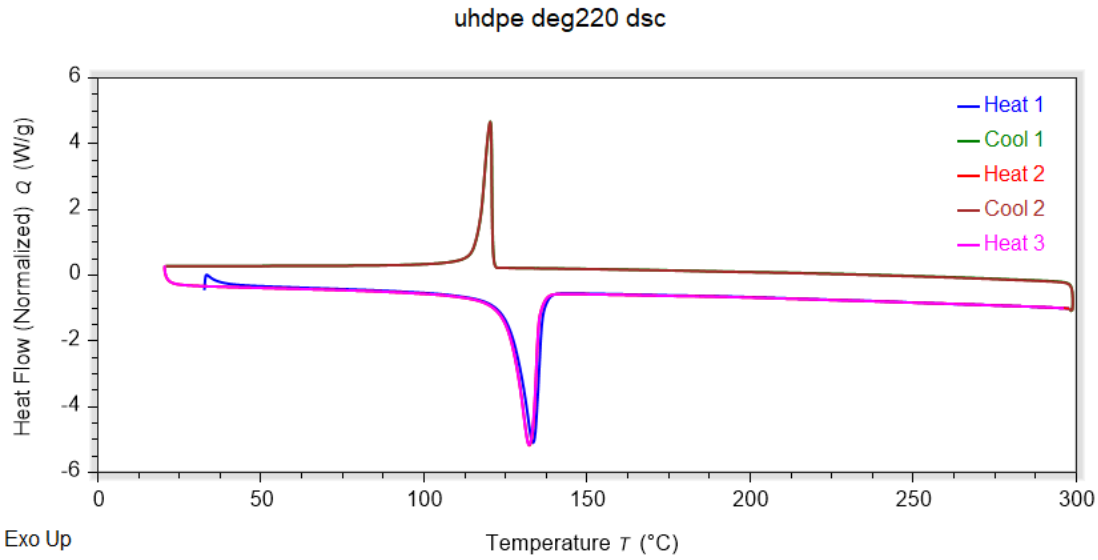

Figure 34

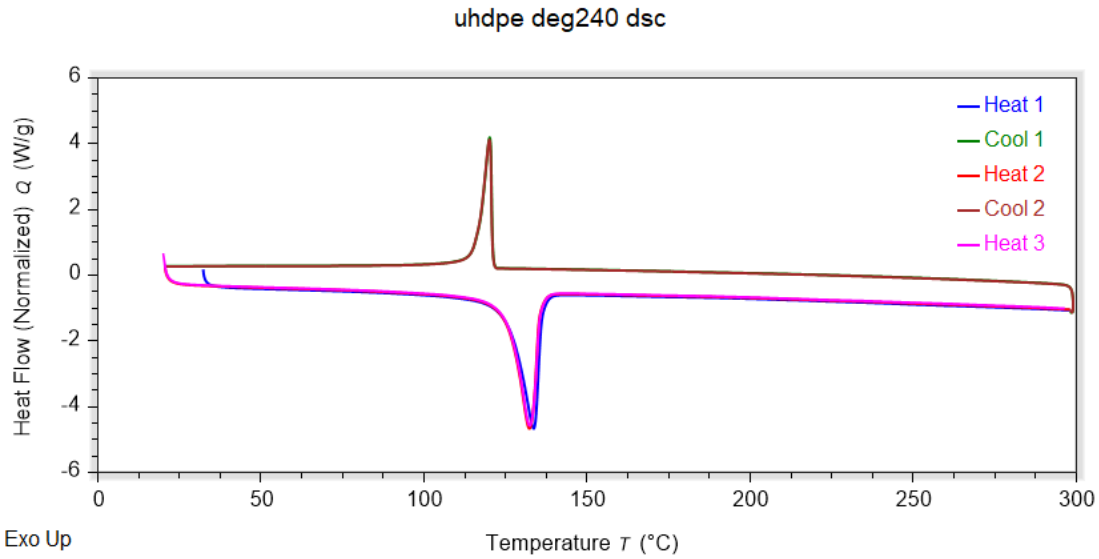

Figure 35

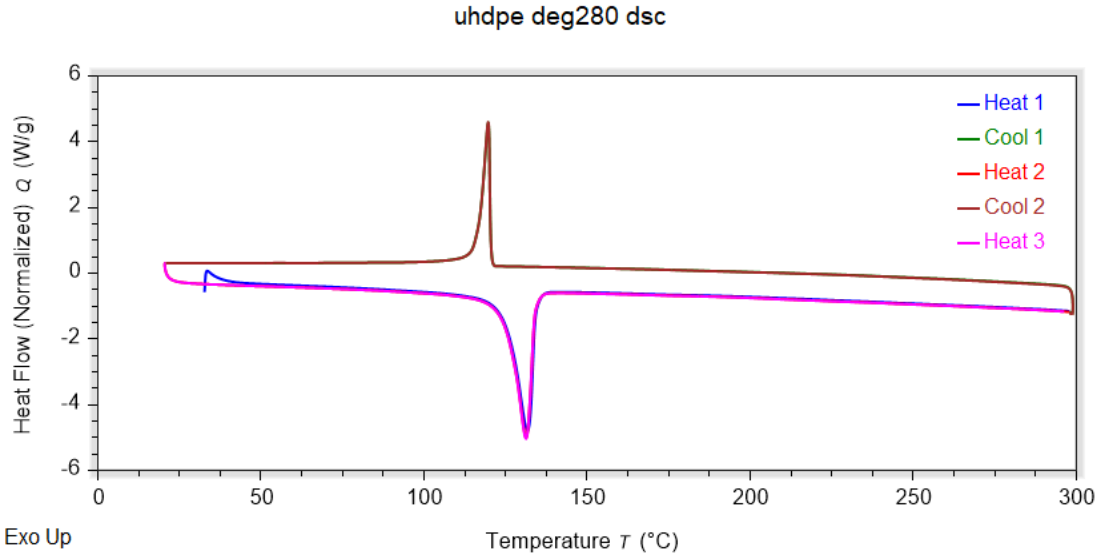

Figure 36

Full OIT scans

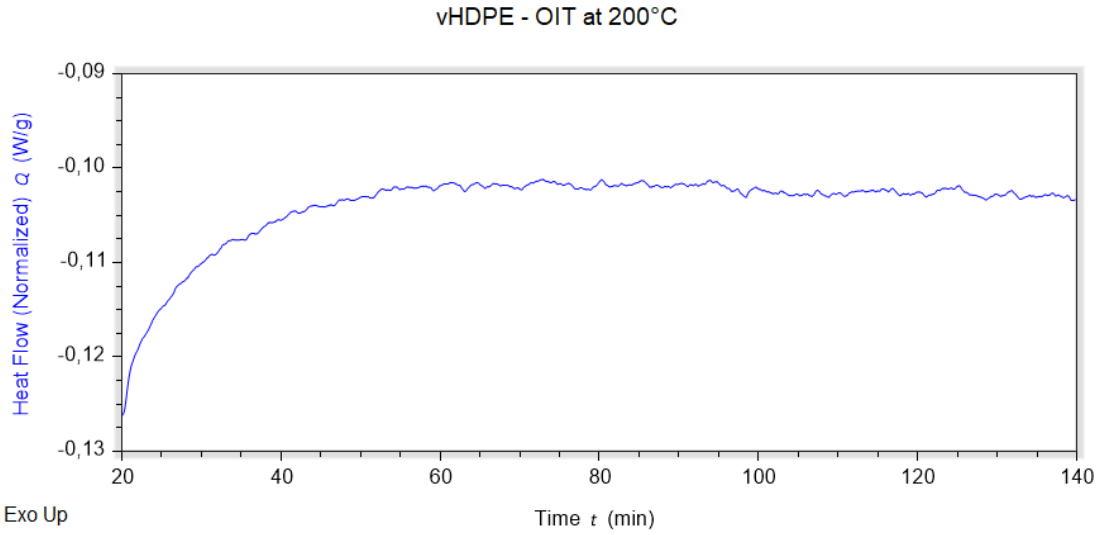

Figure 37

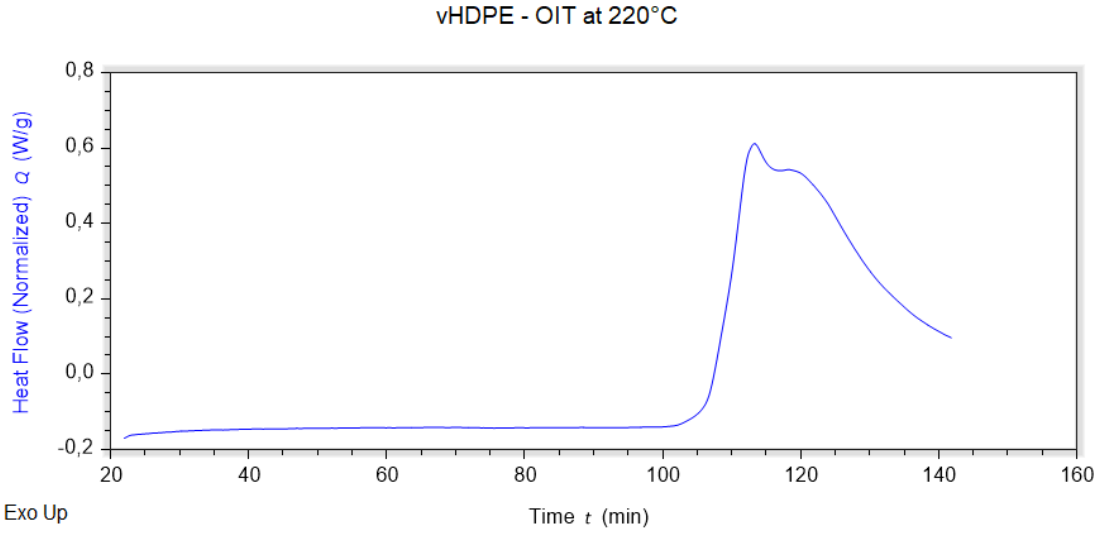

Figure 38

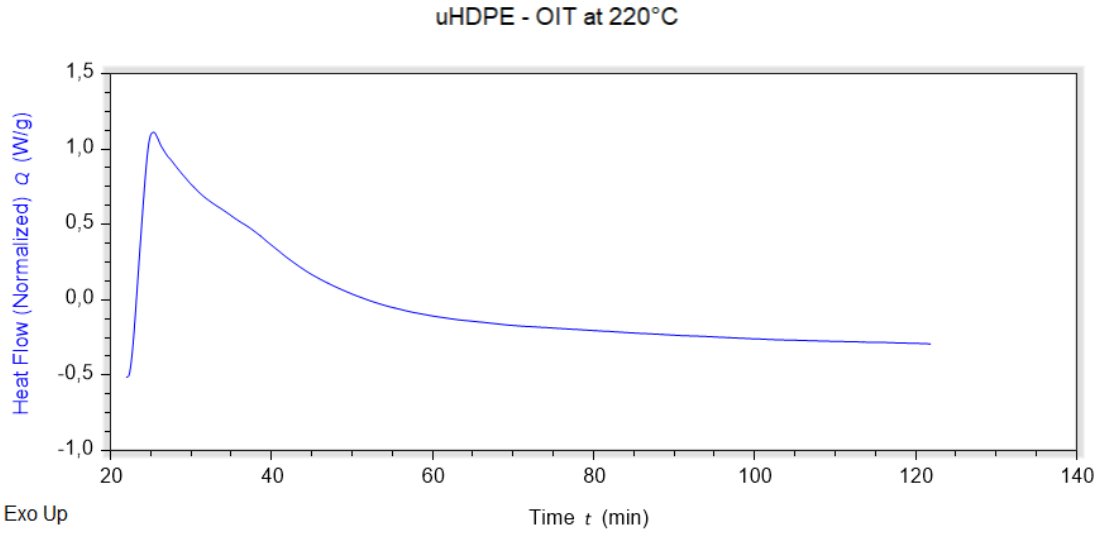

Figure 39

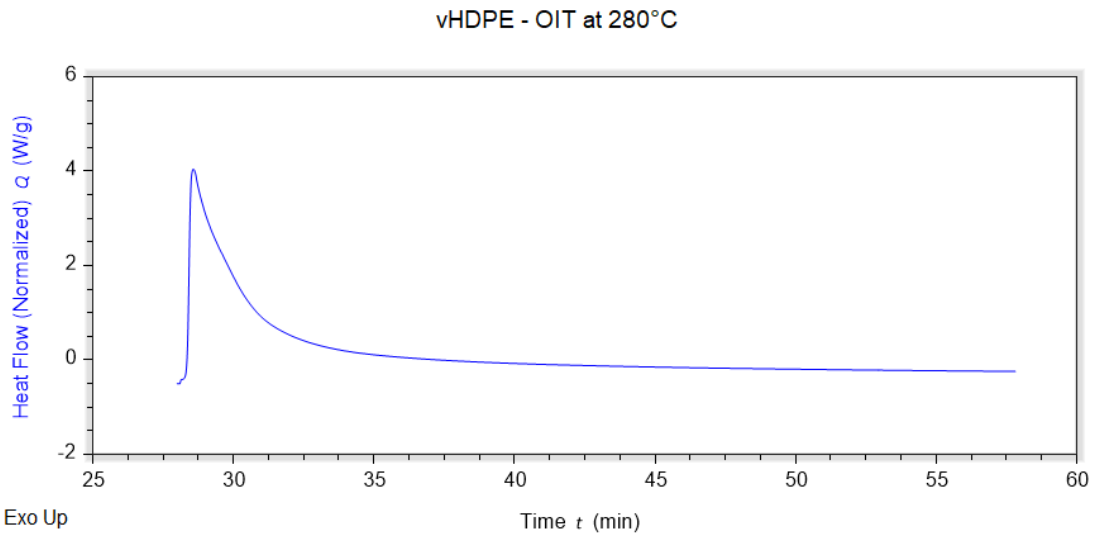

Figure 40

A.2 Rheology

Objective

Perform frequency sweeps on virgin, degraded and regrinded HDPE in order to find parameters that give a wide range of frequencies to the right of the crossover point. 2 frequencies are needed beyond the crossover point for testing with different frequencies in amplitude sweeps

Hypothesis

Lower temperatures should shift the crossover point to the left, enabling more possible frequency choices for the amplitude sweep.

Materials and Methods

AR-G2 rheometer from TA instruments

virgin HDPE

regrind HDPE

Material left on plate to melt for 3 minutes before approaching trim gap.

Degradation study of virgin HDPE - plates heated to 280 °C, material left on plate for 30 minutes, temperature decreased to 200, approach trim gap.

Trim gap: 785 μm

Geometry gap: 750 μm

Test sequences

1. Preliminary amplitude sweeps of virgin and regrind
    - test for gap size and temperature
    - Performed at 220-250 °C
2. Frequency sweeps of virgin, regrind and virgin degraded
    - test temperatures (160 °C - 200°C)
    - find test temperature where crossover point is as far left as possible
    - **200°C chosen - compromise between preparation time and crossover point**
3. Amplitude sweeps of virgin, regrind and virgin degraded
    - Test at 8Hz and 2Hz until 400% strain
    - Find amplitude sweep crossover point and compare location for frequencies and materials

Full amplitude sweeps from main report

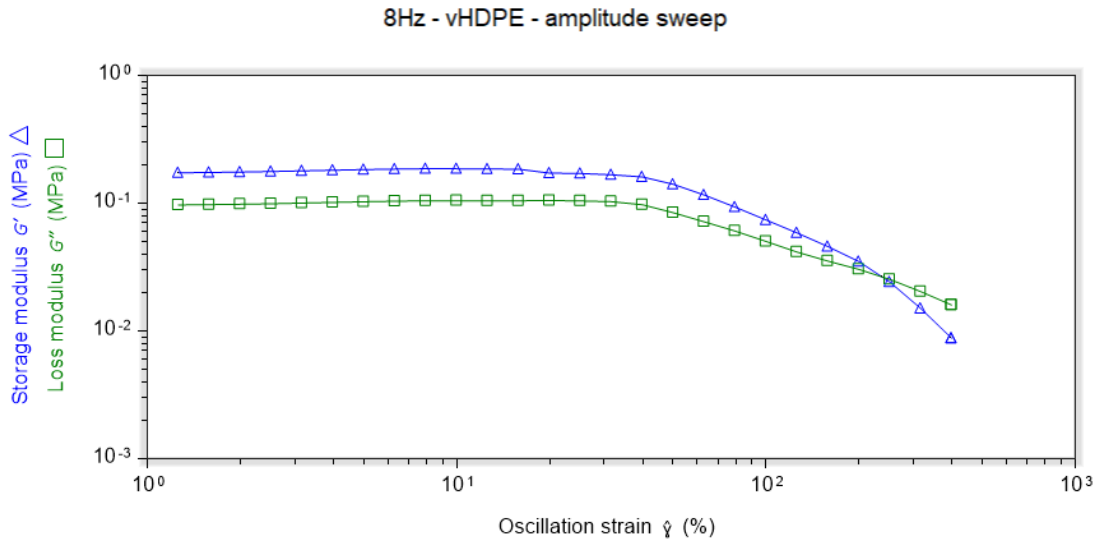

Figure 41: Amplitude sweep at 8Hz frequency vHDPE

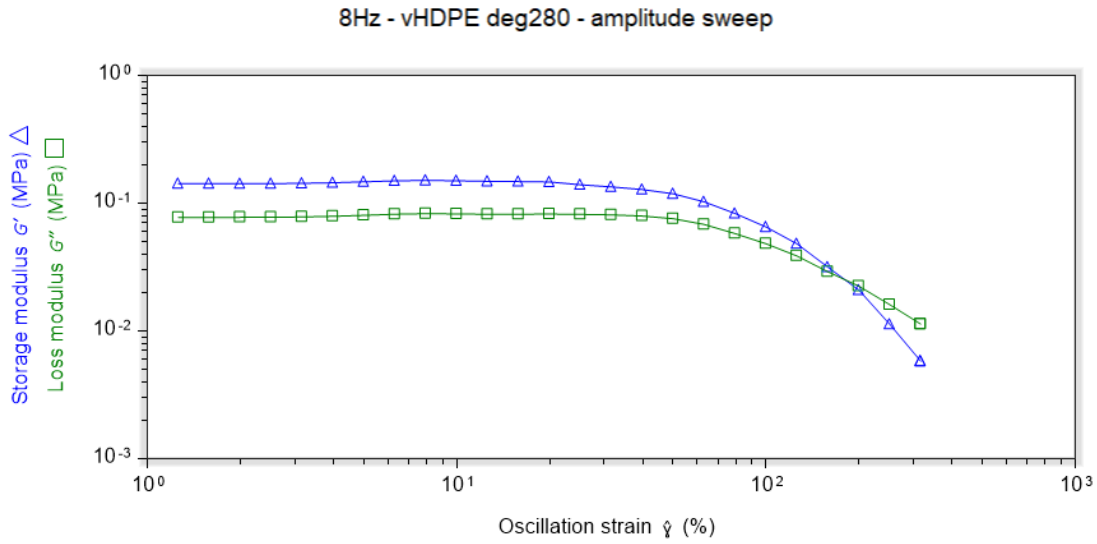

Figure 42: Amplitude sweep at 8Hz frequency vHDPEdeg280

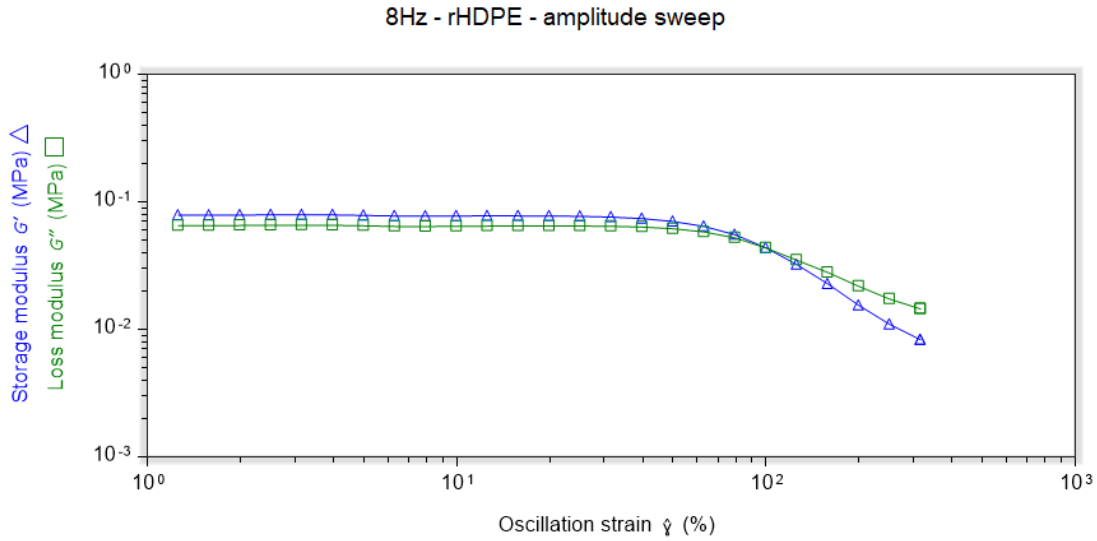

Figure 43: Amplitude sweep at 8Hz frequency rHDPE

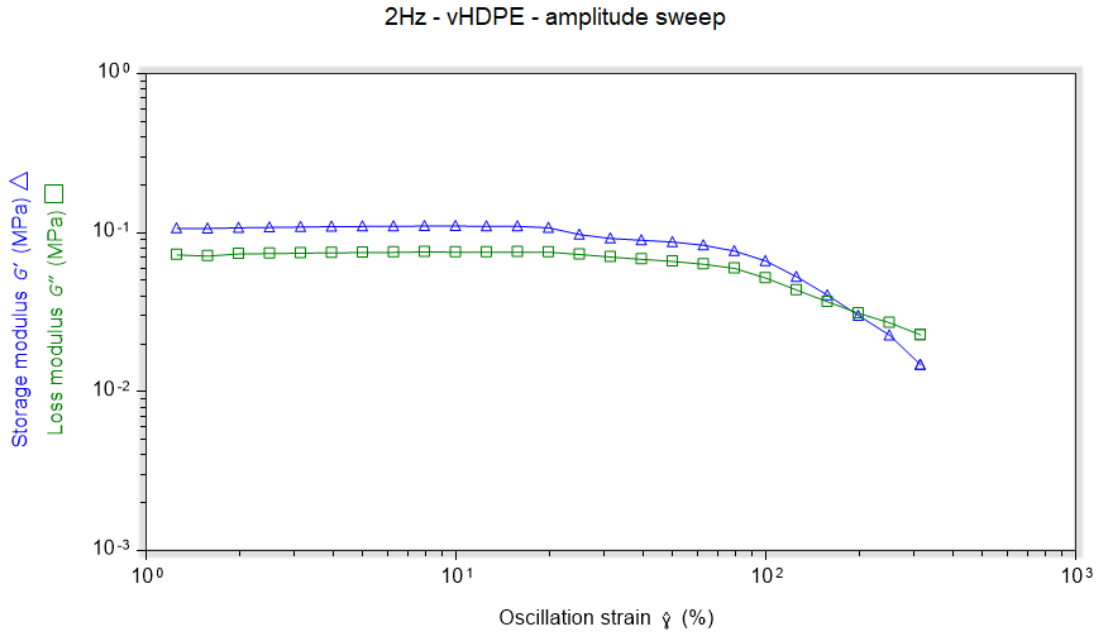

Figure 44: Amplitude sweep at 2Hz frequency vHDPE

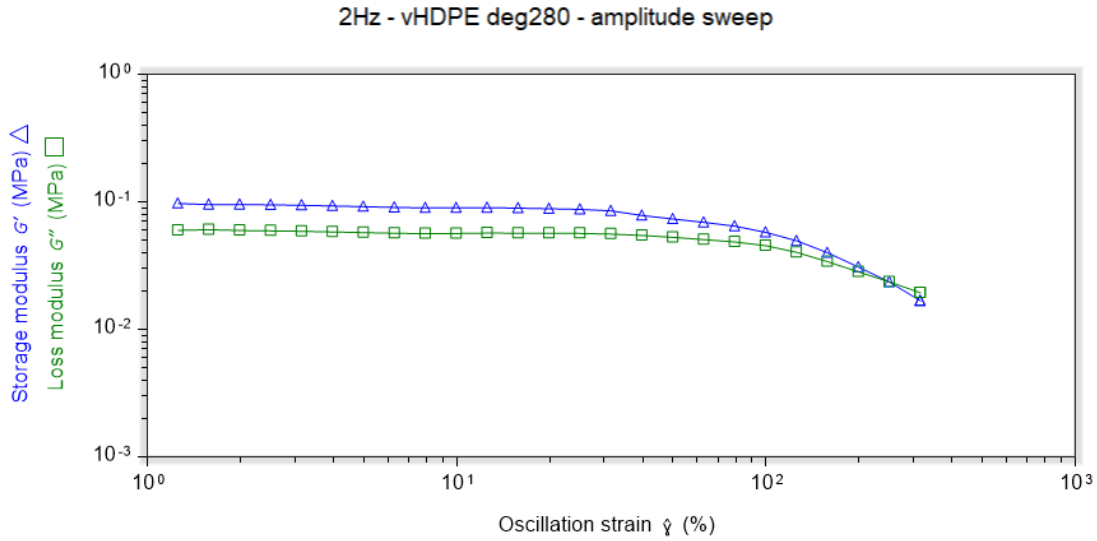

Figure 45: Amplitude sweep at 2Hz frequency vHDPEdeg280

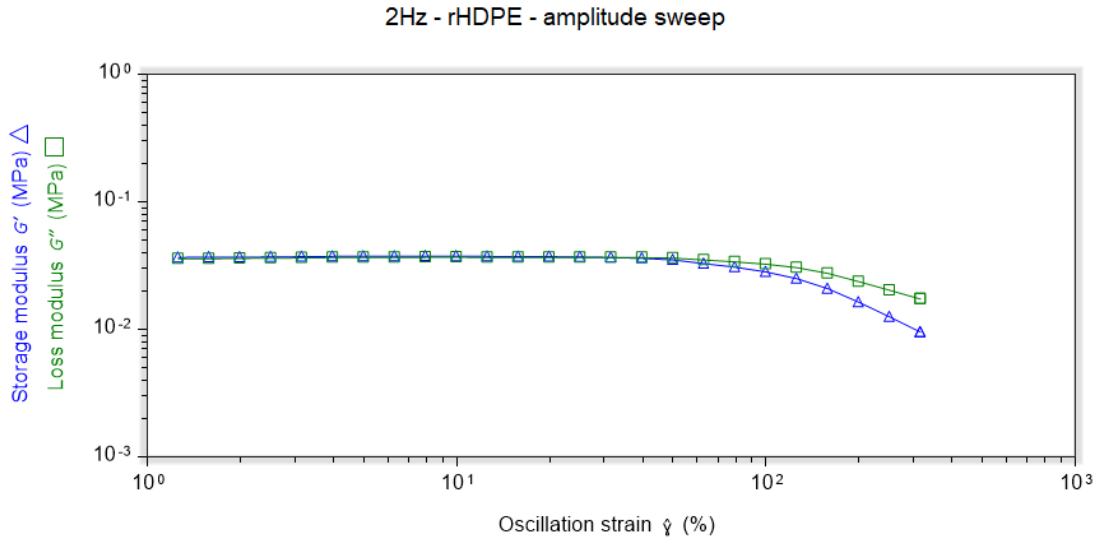

Figure 46: Amplitude sweep at 2Hz frequency rHDPE

Preliminary frequency sweeps at different temperatures

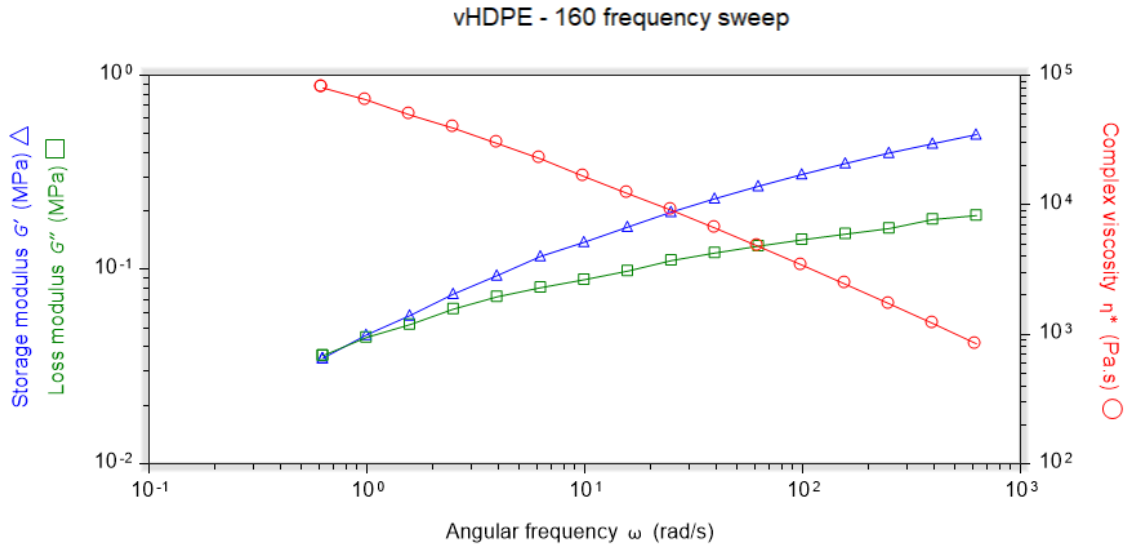

Figure 47: 160°C vHDPE

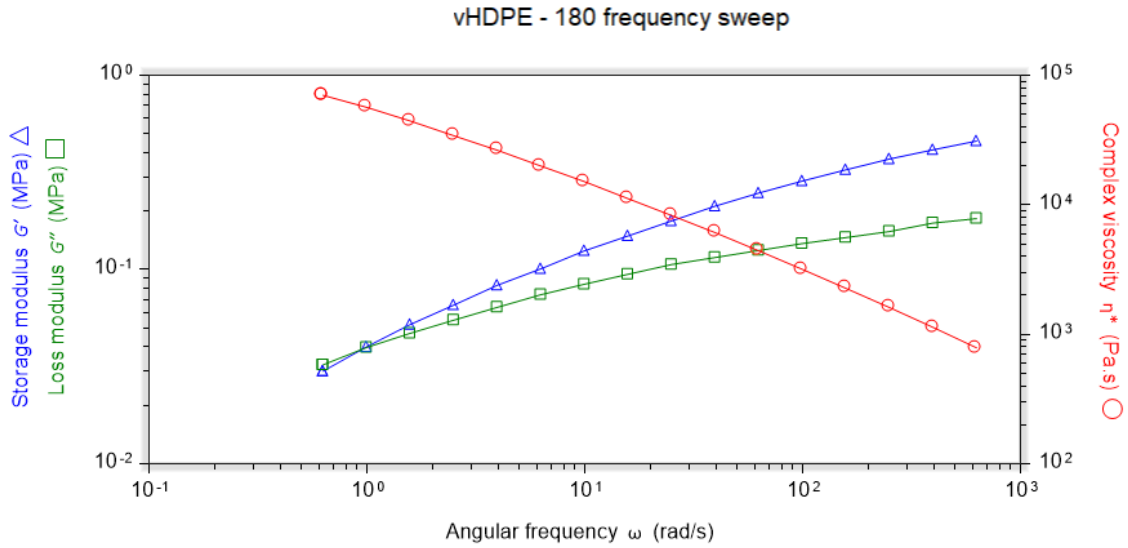

Figure 48: 180°C vHDPE

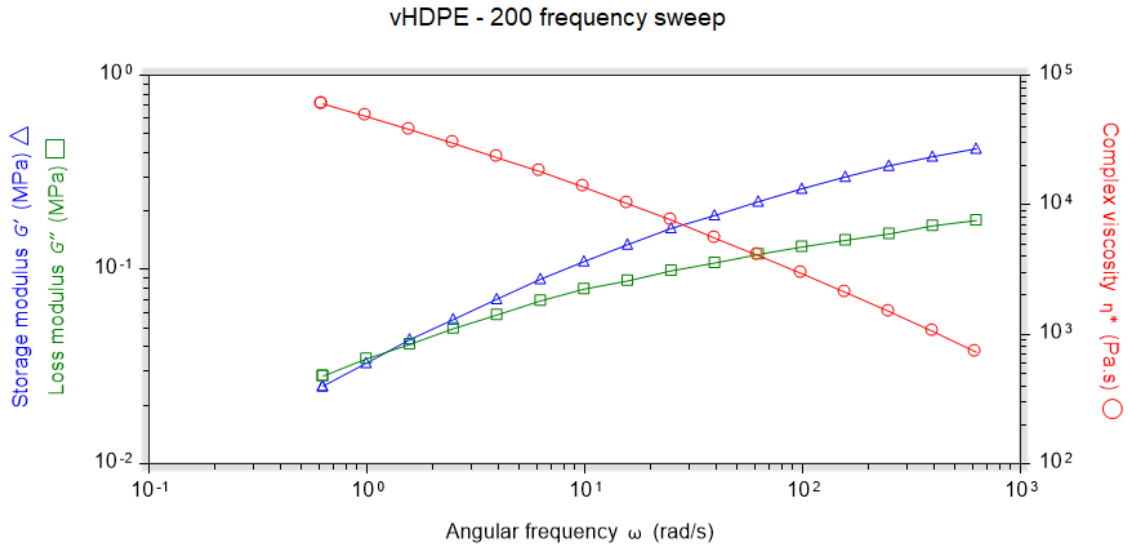

Figure 49: 200°C vHDPE

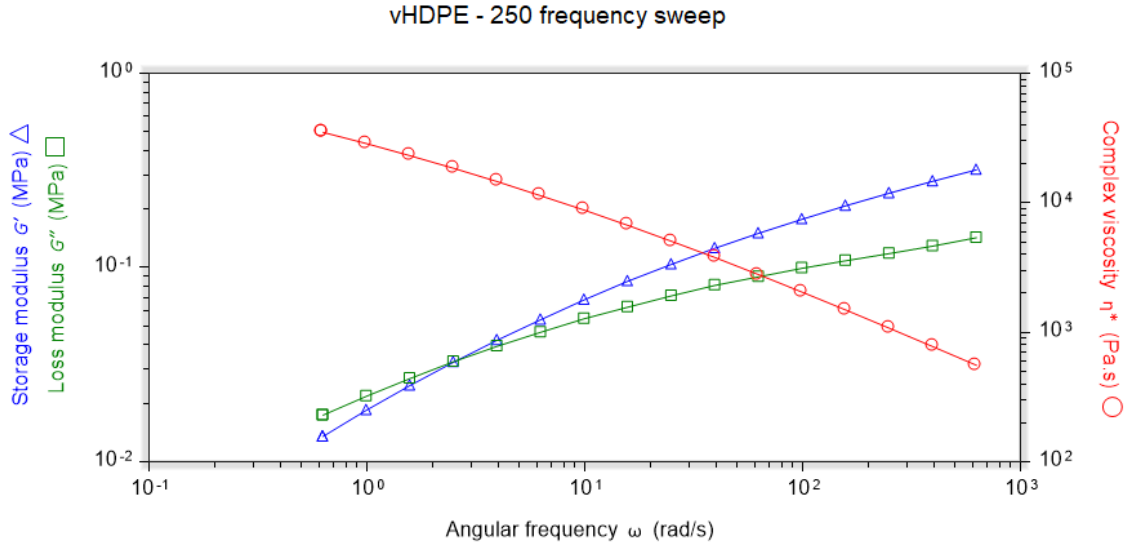

Figure 50: 250°C vHDPE

Full Lissajous Bowditch plots from main report

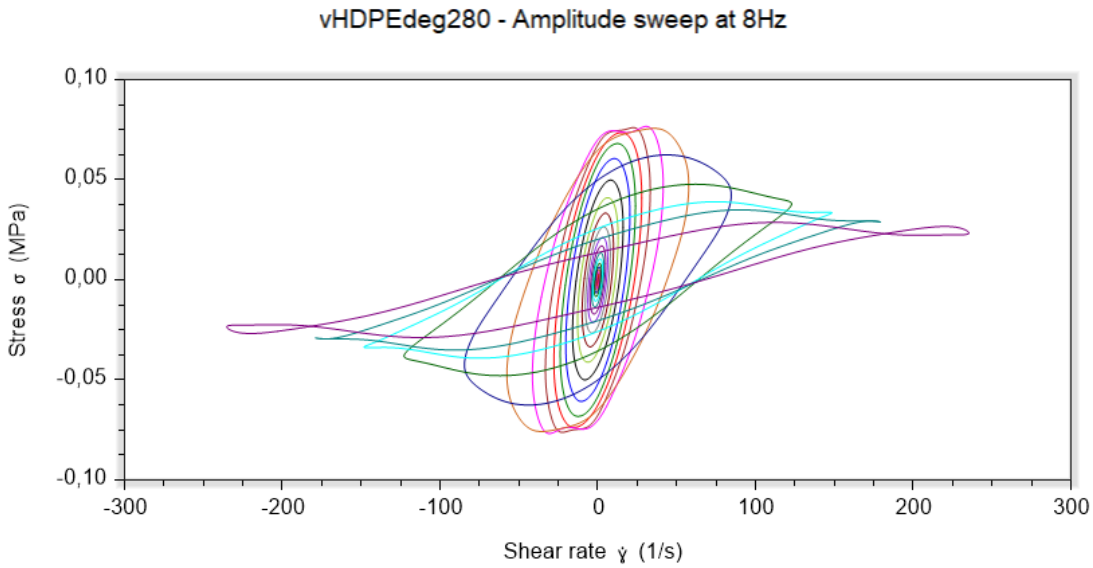

Figure 51: Lissajous-Bowditch vHDPEdeg280 8Hz

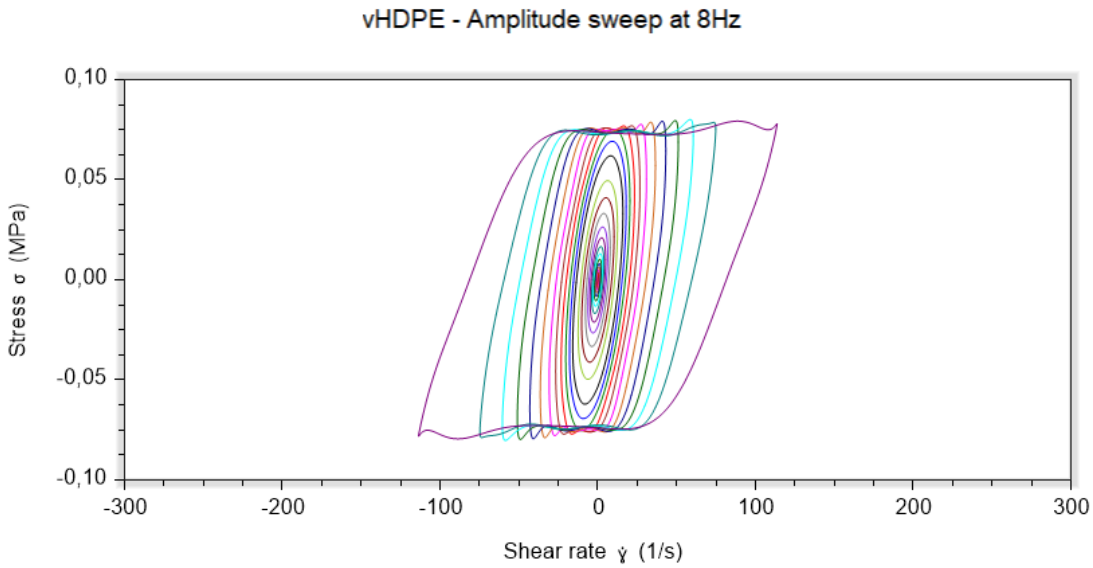

Figure 52: Lissajous-Bowditch vHDPE 8Hz

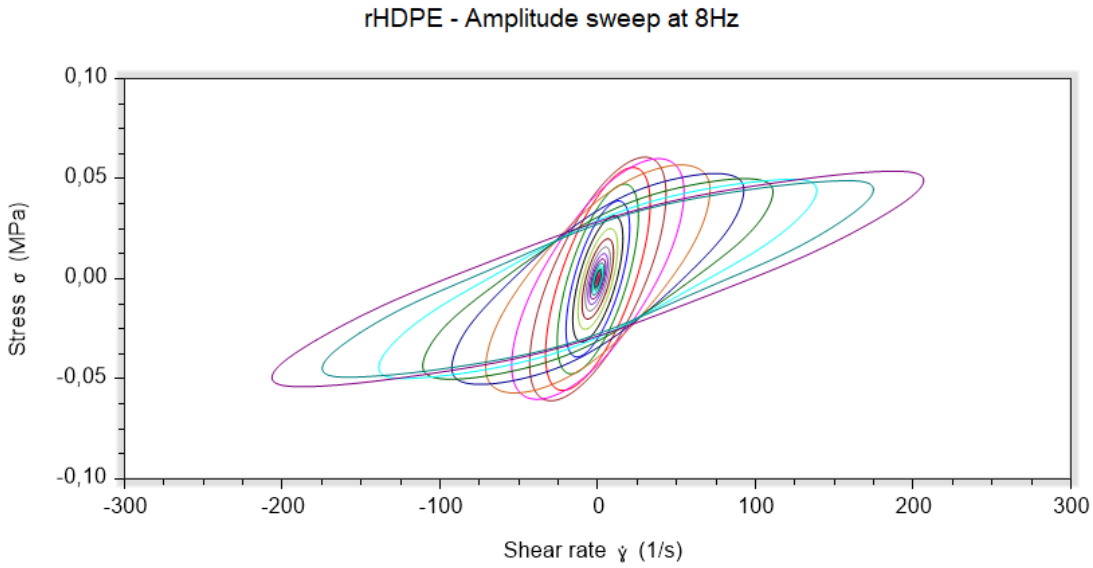

Figure 53: Lissajous-Bowditch rHDPE 8Hz

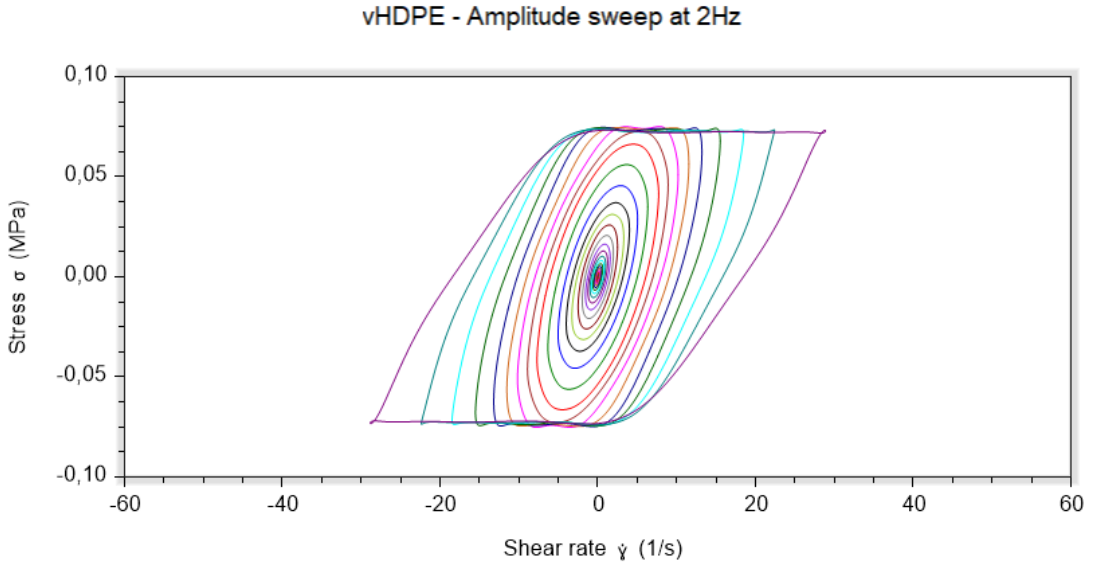

Figure 54: Lissajous-Bowditch vHDPE 2Hz

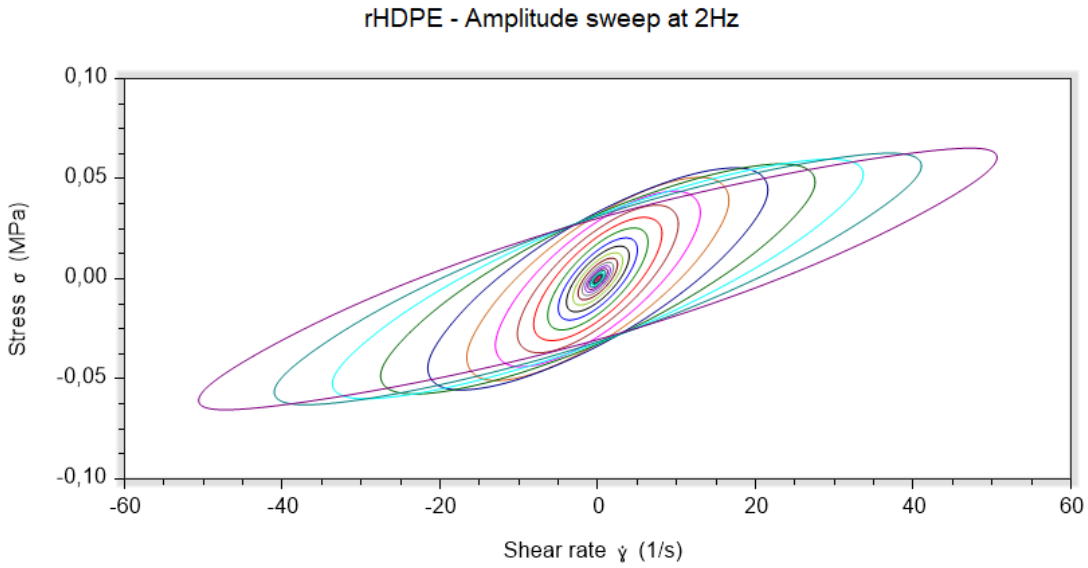

Figure 55: Lissajous-Bowditch rHDPE 2Hz

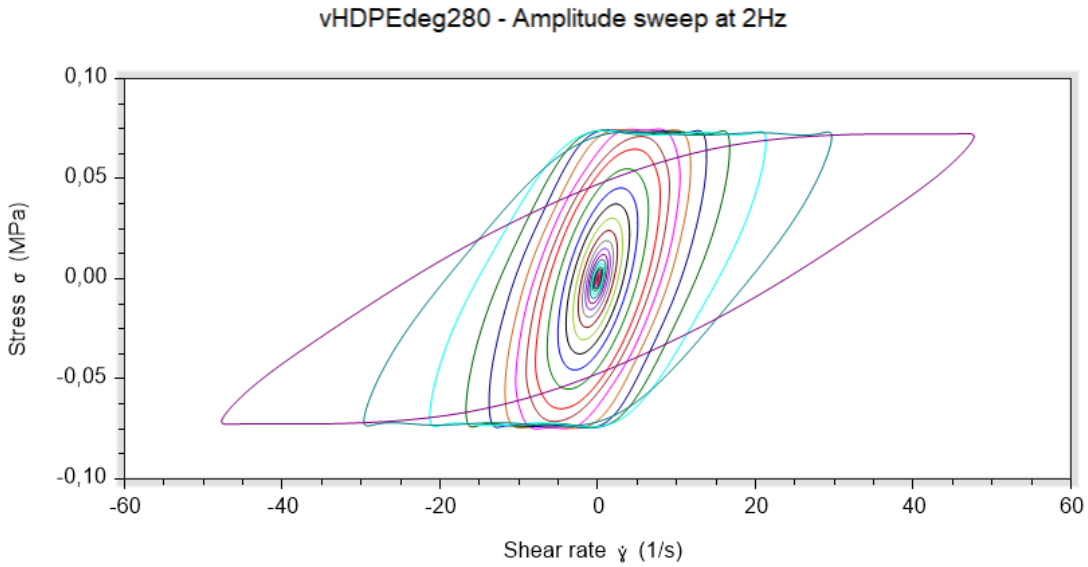

Figure 56: Lissajous-Bowditch vHDPEdeg280 2Hz

A.3 Structural analysis

SEM

[63] studying banded spherulites in HDPE by electron microscopy

- challenging sample preparation
- sample prep artifacts can occur at any step - enhanced risk w/ scratches, fractures or impurities

[27] - Morphology of undeformed and deformed polyethylene lamellar crystals

- smooth surfaces for etching revealed by cutting with microtome and freshly prepared glass or diamond knife at room temperature

Methods for etching described in [59] use rapid xylene etching to reveal spherulites in polyethylene. Benzene was also successfully used as an etching solution for polyethylene. Staining with chlorosulfonic acid additionally enhanced the visibility of lamellar structures in polyethylene, attributed to the crosslinking caused by the method, which stains the amorphous regions by selective diffusion, enabling thin sectioning for SEM analysis.

X-ray

WAXS and SAXS give complementary information on the crystalline structures and lamellar spacings [44]. Cazenave et al. [13] investigated SAXS of HDPE and found a correlation between crystallization kinetics and chain structure. An analysis of the lamellar thickness and crystallinity of HDPE by SAXS and WAXS, with comparison to degree of crystallinity and lamellar thickness from DSC was conducted in [15], revealing comparable results of the methods.

A.4 Repeatability of experimental results

TGA

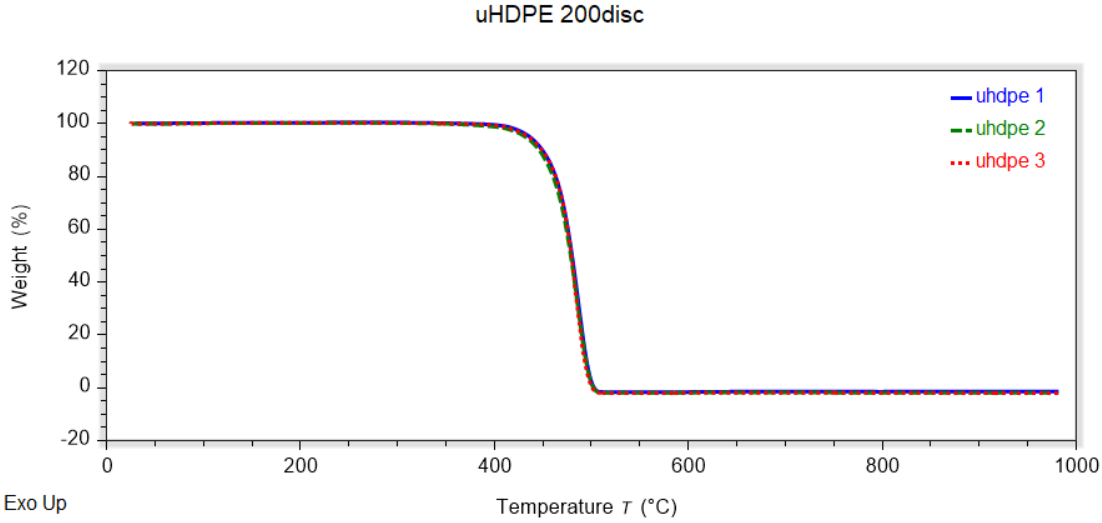

Figure 57: Repeatability of TGA - uHDPE

Rheology

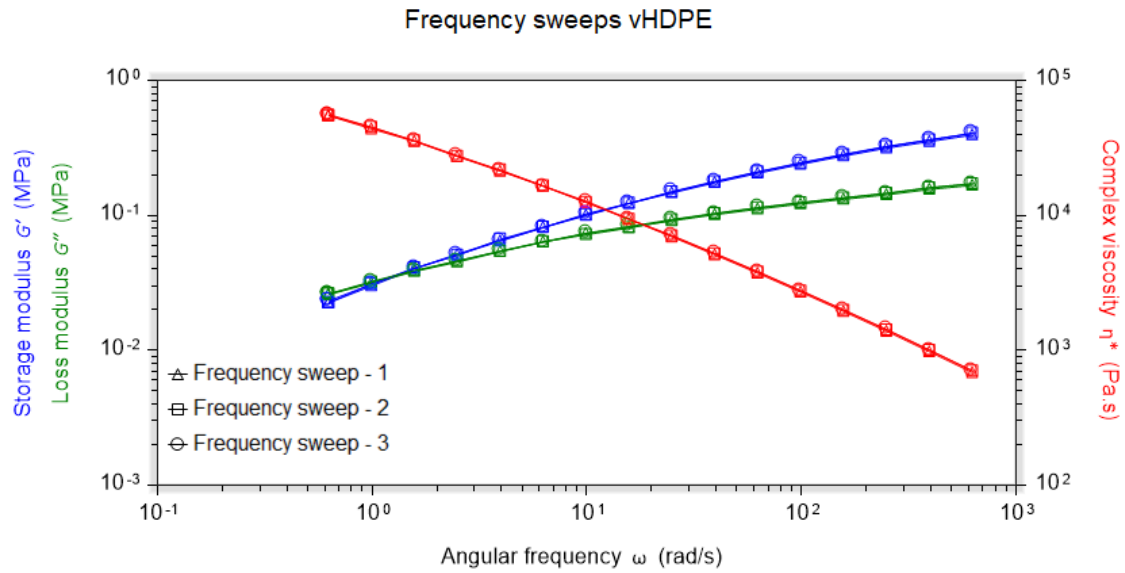

Figure 58: Repeatability of rheological frequency sweeps - vHDPE

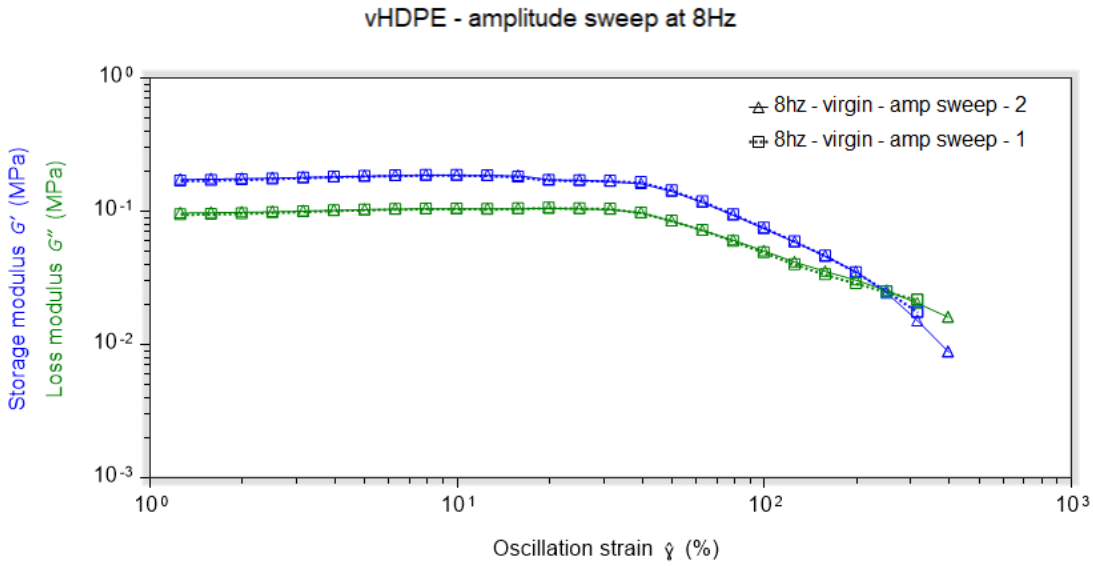

Figure 59: Repeatability of amplitude sweeps - vHDPE

Bibliography

[1] J. Aho. *Rheological Characterization of Polymer Melts in Shear and Extension: Measurement Reliability and Data for Practical Processing.* PhD thesis, Tampere University of Technology, 2011.

[2] S.-M. Alavifar, M. S. Hosseini, and M. K. R. Aghjeh. Effect of carbon black incorporation methods on the initial creep/slow crack growth resistance and properties of high-density polyethylene (hdpe) pipes. *Materials today communications*, 39, 2024. ISSN 2352-4928.

[3] M. Alzerreca, M. Paris, O. Boyron, D. Orditz, G. Louarn, and O. Correc. Mechanical properties and molecular structures of virgin and recycled HDPE polymers used in gravity sewer systems. *Polymer Testing*, 46:1 – 8, 2015. doi: 10.1016/j.polymertesting.2015.06.012.

[4] F. M. Andersen, A. Giannas, and M. H. Mikkelsen. Characterization of properties of virgin and recycled high-density polyethylene under cyclic loading. *Aalborg University student report*, 2023.

[5] E. H. Andrews and B. J. Walker. Fatigue fracture in polyethylene. *Proceedings of the Royal Society of London. Series A, Mathematical and Physical Sciences*, 325(1560):57–79, 1971. ISSN 00804630.

[6] R. F. Baddour, A. S. Michaels, H. J. Bixler, R. P. De Filippi, and J. A. Barrie. Transport of liquids in structurally modified polyethylene. *Journal of Applied Polymer Science*, 8(2):897–933, 1964. doi: https://doi.org/10.1002/app.1964.070080229.

[7] Z. Bartczak and M. Kozanecki. Influence of molecular parameters on high-strain deformation of polyethylene in the plane-strain compression. part I. stress–strain behavior. *Polymer*, 46(19):8210–8221, 2005. ISSN 0032-3861. doi: https://doi.org/10.1016/j.polymer.2005.06.100. Controlled Macromolecular Synthesis and Controlled Architectures - Supramolecular Polymer Assemblies.

[8] Z. Bartczak and A. Vozniak. WAXS/SAXS study of plastic deformation instabilities and lamellae fragmentation in polyethylene. *Polymer*, 177:160–177, 2019. ISSN 0032-3861. doi: https://doi.org/10.1016/j.polymer.2019.05.076.

[9] R. L. Blaine. Thermal applications note: Polymer heats of fusion. URL `https://www.tainstruments.com/pdf/literature/TN048.pdf`.

[10] Borealis. Polyethylene BorSafe™ HE3490-LS, 2008. URL `https://www.borealisgroup.com/storage/Datasheets/HE3490-LS-IBD_MSDS-REG_EUROPE-EN-V13-ZPDS-EUR-37130-10018956.pdf`.

[11] M. Bourchak and A. Aid. PE-HD fatigue damage accumulation under variable loading based on various damage models. *Express Polymer Letters*, 11:117–126, 02 2017. doi: 10.3144/expresspolymlett.2017.13.

[12] W. D. Callister and D. G. Rethwisch. *Materials Science and Engineering*. Wiley & Sons, ninth edition, 2015. ISBN 978-1-118-31922-2.

[13] J. Cazenave, R. Seguela, B. Sixou, and Y. Germain. Short-term mechanical and structural approaches for the evaluation of polyethylene stress crack resistance. *Polymer (Guilford)*, 47(11):3904–3914, 2006. ISSN 0032-3861.

[14] T. T. Chen. Using the large amplitude oscillatory shear (LAOS) method to characterize polymer long chain branching. URL `https://www.tainstruments.com/pdf/literature/RT006.pdf`.

[15] J. J. Cheng, M. A. Polak, and A. Penlidis. Phase interconnectivity and environmental stress cracking resistance of polyethylene: A crystalline phase investigation. *Journal of Macromolecular Science, Part A*, 46(6):572–583, 2009. doi: 10.1080/10601320902851801.

[16] J. J. Cheng, M. A. Polak, and A. Penlidis. Influence of micromolecular structure on environmental stress cracking resistance of high density polyethylene. *Tunnelling and underground space technology*, 26(4):582–593, 2011. ISSN 0886-7798.

[17] J. C. Cruz and J. A. Jansen. Environmental stress cracking. In *Characterization and Failure Analysis of Plastics*. ASM International, 05 2022. ISBN 978-1-62708-395-9. doi: 10.31399/asm.hb.v11B.a0006917.

[18] S. Cruz and M. Zanin. Evaluation and identification of degradative processes in post-consumer recycled high-density polyethylene. *Polymer degradation and stability*, 80(1):31–37, 2003. ISSN 0141-3910.

[19] A. Cuadri and J. Martín-Alfonso. The effect of thermal and thermo-oxidative degradation conditions on rheological, chemical and thermal properties of hdpe. *Polymer degradation and stability*, 141:11–18, 2017. ISSN 0141-3910.

[20] M. Dahl and R. H. Jermiin. Comparative study on mechanical properties of virgin and recycled high density polyethylene. *Aalborg University student report*, 2019.

[21] S. Deveci, N. Antony, and B. Eryigit. Effect of carbon black distribution on the properties of polyethylene pipes - part 1: Degradation of post yield mechanical properties and fracture surface analyses. *Polymer degradation and stability*, 148:75–85, 2018. ISSN 0141-3910.

[22] A. Drozdov and J. deClaville Christiansen. Viscoelasticity and viscoplasticity of semicrystalline polymers: Structure–property relations for high-density polyethylene. *Computational Materials Science*, 39(4):729–751, 2007. ISSN 0927-0256. doi: https://doi.org/10.1016/j.commatsci.2006.09.001.

[23] A. D. Drozdov, J. deClaville Christiansen, and R. H. Jermiin. Lifetime predictions for high-density polyethylene under creep: Experiments and modeling. *Polymers.*, 15(2), 2023-1-09. ISSN 2073-4360.

[24] A. D. Drozdov, R. H. Jermiin, and J. deClaville Christiansen. Lifetime predictions for virgin and recycled high-density polyethylene under creep conditions. 2024. doi: https://doi.org/10.48550/arXiv.2404.10336.

[25] DS/EN ISO 11357-6:2018. *Plastics – Differential scanning calorimetry (DSC) – Part 6: Determination of oxidation induction time (isothermal OIT) and oxidation induction temperature (dynamic OIT)*. International Organization for Standardization, Brussels, 2018.

[26] C. D. C. Erbetta, G. F. Manoel, A. P. L. R. Oliveira, M. E. S. R. e. Silva, R. F. S. Freitas, and R. G. Sousa. Rheological and thermal behavior of high-density polyethylene (hdpe) at different temperatures. *Materials sciences and applications*, 5(13):923–931, 2014. ISSN 2153-117X.

[27] A. Galeski, Z. Bartczak, T. Kazmierczak, and M. Slouf. Morphology of undeformed and deformed polyethylene lamellar crystals. *Polymer (Guilford)*, 51(24):5780–5787, 2010. ISSN 0032-3861.

[28] W. Ghabeche and K. Chaoui. Surface Degradation and Crystallinity Changes in HDPE-100 Pipe Subjected to Chemical Aggressive Environments. In A. F. de Mécanique, editor, *CFM 2013 - 21ème Congrès Français de Mécanique*, Congrès français de mécanique, Bordeaux, France, 2013. AFM, Maison de la Mécanique, 39/41 rue Louis Blanc - 92400 Courbevoie. URL `https://hal.science/hal-03440583`. Colloque avec actes et comité de lecture. Internationale.

[29] A. Gobetti and G. Ramorino. Application of short-term methods to estimate the environmental stress cracking resistance of recycled HDPE. *Journal of polymer research*, 27(11), 2020. ISSN 1022-9760.

[30] J. Gulmine, P. Janissek, H. Heise, and L. Akcelrud. Degradation profile of polyethylene after artificial accelerated weathering. *Polymer Degradation and Stability*, 79(3):385–397, 2003. ISSN 0141-3910. doi: https://doi.org/10.1016/S0141-3910(02)00338-5.

[31] Q. Guo. Part ii: Morphology, properties, and processing. In *Polymer Morphology*. John Wiley & Sons, Incorporated, United States, 2016. ISBN 9781118892770.

[32] S. O. Han, D. W. Lee, and O. H. Han. Thermal degradation of crosslinked high density polyethylene. *Polymer Degradation and Stability*, 63(2):237–243, 1999. ISSN 0141-3910. doi: https://doi.org/10.1016/S0141-3910(98)00098-6.

[33] C. Harper. *Modern Plastics Handbook*. McGraw-Hill handbooks. Mcgraw-hill, 2000. ISBN 9780070267145.

[34] A. Holmström and E. Sörvik. Thermal degradation of polyethylene in a nitrogen atmosphere of low oxygen content. iv. structural changes occurring in different types of high-density polyethylene. *Journal of Polymer Science: Polymer Symposia*, 57:33–53, 2007. doi: 10.1002/POLC.5070570106.

[35] A. Holmström and E. M. Sörvik. Thermooxidative degradation of polyethylene. i and ii. structural changes occurring in low-density polyethylene, high-density polyethylene, and tetratetracontane heated in air. *Journal of Polymer Science: Polymer Chemistry Edition*, 16 (10):2555–2586, 1978. doi: https://doi.org/10.1002/pol.1978.170161012.

[36] L. Hubert, L. David, R. Seguela, G. Vigier, C. Degoulet, and Y. Germain. Physical and mechanical properties of pe for pipes in relation to molecular architecture . part i : Microstructure and crystalization kinetics. *Polymer (Guilford)*, pages 8425–8434, 2001. ISSN 0032-3861.

[37] I. O. Igwe. Uptake of aromatic solvents by polyethylene films. *Journal of Applied Polymer Science*, 104(6):3849–3854, 2007. doi: https://doi.org/10.1002/app.25980.

[38] S. O. Ilyin, A. Y. Malkin, and V. G. Kulichikhin. Application of large amplitude oscillatory shear for the analysis of polymer material properties in the nonlinear mechanical behavior. *Polymer science. Series A, Chemistry, physics*, 56(1):98–110, 2014. ISSN 0965-545X.

[39] R. S. Jeyaseelan and A. Giacomin. Structural network theory for a filled polymer melt in large amplitude oscillatory shear. *Polymer gels and networks*, 3(2):117–133, 1995. ISSN 0966-7822.

[40] N.-J. Jo, A. Takahara, and T. Kajiyama. Effect of aggregation structure on non-linear dynamic viscoelastic characteristics of oriented high-density polyethylenes under cyclic fatigue. *Polymer (Guilford)*, 38(20):5195–5201, 1997. ISSN 0032-3861.

[41] T. Kealy. Rheological analysis of the degradation of hdpe during consecutive processing steps and for different processing conditions. *Journal of Applied Polymer Science*, 112(2): 639–648, 2009. doi: https://doi.org/10.1002/app.29418.

[42] J. C.-W. Lee, L. Porcar, and S. A. Rogers. Unveiling temporal nonlinear structure–rheology relationships under dynamic shearing. *Polymers*, 11(7), 2019. ISSN 2073-4360. doi: 10.3390/polym11071189. URL `https://www.mdpi.com/2073-4360/11/7/1189`.

[43] A. Lustiger and R. Markham. Importance of tie molecules in preventing polyethylene fracture under long-term loading conditions. *Polymer (Guilford)*, 24(12):1647–1654, 1983. ISSN 0032-3861.

[44] J. E. Mark. *Physical Properties of Polymers Handbook*. Springer New York, New York, NY, 2nd ed. 2007. edition, 2007. ISBN 1-280-81656-2.

[45] A. Mendes, A. Cunha, and C. Bernardo. Study of the degradation mechanisms of polyethylene during reprocessing. *Polymer degradation and stability*, 96(6):1125–1133, 2011. ISSN 0141-3910.

[46] T. J. Menna. *Characterization and Failure Analysis of Plastics*. ASM International, 05 2022. ISBN 978-1-62708-395-9. doi: 10.31399/asm.hb.v11B.9781627083959.

[47] T. G. Mezger. *The Rheology Handbook: 4th Edition*. Vincentz Network, Germany, 2012. ISBN 9783748600367.

[48] J. Molnár, Z. Zuba, Ö. Sepsi, F. Ujhelyi, G. Erdei, S. Lenk, and A. Menyhárd. Structural investigation of semicrystalline polymers. *Polymer Testing*, 95:107098, 2021. ISSN 0142-9418. doi: https://doi.org/10.1016/j.polymertesting.2021.107098.

[49] A. B. D. Nandiyanto, R. Oktiani, and R. Ragadhita. How to read and interpret FTIR spectroscope of organic material. *Indonesian journal of science and technology*, 4(1):97–, 2019. ISSN 2528-1410.

[50] P. Oblak, J. Gonzalez-Gutierrez, B. Zupančič, A. Aulova, and I. Emri. Processability and mechanical properties of extensively recycled high density polyethylene. *Polymer Degradation and Stability*, 114:133–145, 2015. ISSN 0141-3910. doi: https://doi.org/10.1016/j.polymdegradstab.2015.01.012.

[51] T. A. Osswald and G. Menges. *Materials Science of Polymers for Engineers*. Hanser Gardner publications, London, second edition, 2003. ISBN 1569903484.

[52] P. Pagès, F. Carrasco, J. Surina, and X. Colom. FTIR and DSC study of hdpe structural changes and mechanical properties variation when exposed to weathering aging during canadian winter. *Journal of Applied Polymer Science*, 60(2):153–159, 1996. doi: https://doi.org/10.1002/(SICI)1097-4628(19960411)60:2<153::AID-APP2>3.0.CO;2-R.

[53] J. Parameswaranpillai. *Recent Developments in Plastic Recycling*. Composites Science and Technology. Springer Nature Singapore, Singapore, 1st ed. 2021. edition, 2021. ISBN 981-16-3627-3.

[54] J. P. Patel, Y. Schneider, M. Sankarasubramanian, and V. Jayaram. Fundamentals of polymer additives. In *Characterization and Failure Analysis of Plastics*. ASM International, 05 2022. ISBN 978-1-62708-395-9. doi: 10.31399/asm.hb.v11B.a0006939.

[55] Perkin Elmer. Characterization of polymers using TGA, 2011. URL `https://resources.perkinelmer.com/corporate/cmsresources/images/44-132088app_characterizationofpolymersusingtga.pdf`.

[56] L. Pinheiro, M. Chinelatto, and S. Canevarolo. The role of chain scission and chain branching in high density polyethylene during thermo-mechanical degradation. *Polymer Degradation and Stability*, 86(3):445–453, 2004. ISSN 0141-3910. doi: https://doi.org/10.1016/j.polymdegradstab.2004.05.016.

[57] Plastics Europe. Plastics – the fast facts 2023, 2023. URL `https://plasticseurope.org/wp-content/uploads/2023/10/Plasticsthefastfacts2023.pdf`.

[58] Y. Qin, V. Litvinov, W. Chassé, J. Sun, and Y. Men. Environmental stress cracking of polyethylene pipe: Changes in physical structures leading to failure. *Polymer*, 252:124938, 2022. ISSN 0032-3861. doi: https://doi.org/10.1016/j.polymer.2022.124938.

[59] L. C. Sawyer, D. T. Grubb, and G. F. Meyers. Specimen preparation methods. In *Polymer Microscopy*, pages 130–247. Springer New York, New York, NY, 2008. ISBN 9780387726274.

[60] B. A. G. Schrauwen, R. P. M. Janssen, L. E. Govaert, and H. E. H. Meijer. Intrinsic deformation behavior of semicrystalline polymers. *Macromolecules*, 37(16):6069–6078, 2004. ISSN 0024-9297.

[61] X. Shi, J. Wang, S. Stapf, C. Mattea, W. Li, and Y. Yang. Effects of thermo-oxidative aging on chain mobility, phase composition, and mechanical behavior of high-density polyethylene. *Polymer Engineering and Science*, 51:2171–2177, 2011. doi: 10.1002/PEN.21988.

[62] H. G. Sim, K. H. Ahn, and S. J. Lee. Large amplitude oscillatory shear behavior of complex fluids investigated by a network model: a guideline for classification. *Journal of Non-Newtonian Fluid Mechanics*, 112(2):237–250, 2003. ISSN 0377-0257. doi: https://doi.org/10.1016/S0377-0257(03)00102-2.

[63] S. Tantry, D. Anantharaman, B. Thimmappa, and R. Kamalakaran. Studying banded spherulites in hdpe by electron microscopy. *Polymer testing*, 89:106631–, 2020. ISSN 0142-9418.

[64] M. Thuy, M. Pedragosa-Rincón, U. Niebergall, H. Oehler, I. Alig, and M. Böhning. Environmental stress cracking of high-density polyethylene applying linear elastic fracture mechanics. *Polymers*, 14(12):2415–, 2022. ISSN 2073-4360.

[65] Versalis. Eraclene MP 90 U, 2023. URL `https://versalis.eni.com/en-IT/portfolio/polymers-and-intermediates/polyethylene/hdpe/eraclene-mp-90-u.html`.

[66] S. Yin, R. Tuladhar, F. Shi, R. A. Shanks, M. Combe, and T. Collister. Mechanical reprocessing of polyolefin waste: A review. *Polymer engineering and science*, 55(12):2899–2909, 2015. ISSN 0032-3888.

[67] A. T. P. Zahavich, B. Latto, E. Takacs, and J. Vlachopoulos. The effect of multiple extrusion passes during recycling of high density polyethylene. *Advances in polymer technology*, 16 (1):11–24, 1997. ISSN 0730-6679.

[68] A. J. Zattera, H. M. K. Hubert, A. V. C. de Araújo, L. C. Scienza, V. Martins, and L. H. A. Cândido. Comparative study of the degradation of the green hdpe and petrochemical hdpe in the primary recycling. *Materials science forum*, 1012:67–72, 2020. ISSN 0255-5476.

[69] S.-F. Zeng, P. Guo, C.-Y. Hu, and Z.-W. Wang. Effects of mechanical recycling on optical properties and microstructure of recycled high-density polyethylene pellets and bottles. *Journal of Applied Polymer Science*, 140(6):e53446, 2023. doi: https://doi.org/10.1002/app.53446.

[70] S.-F. Zeng, H.-R. Zhang, Z.-K. Li, C.-Y. Hu, and Z.-W. Wang. Effect of mechanical recycling on crystallization, mechanical, and rheological properties of recycled high-density polyethylene and reinforcement based on virgin high-density polyethylene. *Journal of Applied Polymer Science*, 141(11):e55097, 2024. doi: https://doi.org/10.1002/app.55097.

[71] J. Zhang, V. Hirschberg, and D. Rodrigue. Mechanical fatigue of recycled and virgin high-/low-density polyethylene. *Journal of Applied Polymer Science*, 140(2):e53312, 2022. doi: https://doi.org/10.1002/app.53312.